

Answers to the reviewers

Original title:

“Slope stability and rock fall hazard assessment of volcanic tuffs using RPAS and TLS with 2D FEM slope modelling”.

Modified title:

“Slope stability and rock fall hazard assessment of volcanic tuffs using RPAS with 2D FEM slope modelling”.

Answer to the reviewer #1:

Thank you very much for your very positive opinion on the manuscript.

Answers to the reviewer #2:

Thank you very much for your very constructive comments and suggestions. We have considered all of your comments and modified the manuscript accordingly. Please find **your comments in black** and our **answers to your comments in red** below.

April 15, 2017

Dear Editor, dear Authors:

General comment: This manuscript presents an analysis of volcanic tuffs instability along the southern slope of the Sirok Castel hill (Hungary) through multiple remote sensing, field and laboratory techniques. The topic fits the scope of the special issue and might meet the interest of researchers studying landslide hazard and cultural heritage conservation. Having say that, I think that the paper is not ready for publication and needs to be improved.

Specific comments:

1) Even if I am not an English-native speaker, I would recommend an English edit to improve sentence structure and terminology. The text is often difficult to read. Especially, the introduction and the study area description need major rewriting for sense and flow.

Answer: The completely rewritten and revised paper was checked by a native speaker, who corrected the text.

2) The aim of the paper is not clearly stated. In this way, also the conclusion seems to be too general and lacking of the result of the analysis.

Answer: The new version of the paper has been rewritten after considering this review; it became shorter and more focused. We have reformulated our goals. Slope stability analyses are in the focus supported by remotely piloted aerial systems (RPAS) and analyses by finite element methods (FEM). From the original 28 Figures 10 Figures were left (more concise) and some of them were redrawn. The text is more focused on RPAS-based survey and there is a strong link to slope stability analysis. A new figure (Fig. 4) shows the applied methods and these links (flow chart). The slope stability analysis was revised and additional data on the location of studied sections are given. The Results and Discussions were completely rephrased and given in separated chapters. The Conclusion was rewritten.

3) The structure of the manuscript would be improved separating the Discussion section from the Result section. In the actual form, most of the results seem to be not fully described. The authors use too many figures for the description of the results but most of them are not self-explanatory.

Answer: The revised paper contains new structure: we accepted the suggestion of the reviewer. We clearly separated the Results and Discussion sections. In the Materials and Methods section we have swapped the TLS and RPAS sections, intended more focus on RPAS as applied data acquisition and less for TLS as a validation tool.

4) The description of the study area is too general and not clearly organized. Please improve the description and add details about localization, distribution and geometric characteristic (e.g. dimension and geometry of the blocks) of the existent rock fall deposit at the base of the southern slope of the hill (e.g. page 2, line 26). Additionally, add details about the proneness to weathering of the material forming the slope. This might be a key aspect in long-term slope stability. Consider also to discuss this aspect in the text also in relation to the result of the stability analysis. Avoid to make comparison with other rocks (page 3, line 5), simply describe it in detail.

Answer: The geological conditions of the study area and the slopes are described in more details in the revised manuscript. The cross-sections where slope stability was calculated are shown in the revised paper. There are no rock fall deposits at the base of the southern slope. The proneness of the tuff to weathering was emphasized in the revised text, with added new data on the properties and with new references. The comparison with other rocks has been removed from this part of the text. However, it is necessary to emphasize that the studied tuff is very similar to other tuffs in terms of properties and in terms of slope stability.

5) The authors define the RPAS as a tool that (in this case) allow to create a surface model of the study area. In my opinion, this statement does not reflect the real contribution that RPAS bring in mapping and monitoring application and might be interpreted like a “commercial description of the system”. I would suggest, to underline that RPAS are simply “innovative and user friendly” platforms that offer a new sensing perspective (previously reserved only for small scale and/or very expensive investigation; e.g. airborne Lidar), reducing the time and cost of data acquisition. This perspective, or in other words the possibility to bring the camera (or the sensor) at specific positions above/around the object and to take images with specific geometries, as well as the high repeatability, dramatically enlarged applicability of close to mid-range digital and Sfm photogrammetry and surface monitoring in general.

Answer: The entire structure of the paper was changed in terms of RPAS application. RPAS technology was used to capture fine details even of the inaccessible part of the rock cliff. A new part in the new Discussion chapter provides information on the application of RPAS in comparison with TLS and tachimetry, showing the advantages of RPAS. We agree with the reviewer that this technology is “innovative and user friendly” as well as “it offers a new sensing perspective” which can naturally “reduce time and cost”. The acquired imagery was processed by Structure-from-Motion technology which became very common in photogrammetry nowadays. To be able to monitor terrain surfaces, some conversions and GIS modelling were necessary. One of the messages of our paper is that these platforms are suitable for similar tasks but RPAS is better, faster and cheaper. We have reformulated the text.

6) From the manuscript, it is not clear why the authors need to use both the “RPAS” photogrammetry and the TLS survey to reconstruct the topography of the slope. Especially, they state (see section 3.4) that the use of both techniques made the result difficult to manage and a specific post-processing is required to solve the redundancy of the result. Considering that the result of RPAS photogrammetry are comparable to that obtained using the TLS surveys, I would suggest use only topographic data derived from the RPAS photogrammetry for the analysis and eventually use TLS data to locally validate the reconstructed topography. In this case, they might consider change the title in: “RPAS photogrammetry for slope stability analysis in cultural heritage site, Sirok Castel hill, Hungary”.

Answer: We have reformulated the message in order to express that RPAS technology was the primary one and TLS was only used to validate the obtained surface data. The terrain was excellent to crosscheck these two technologies. Following the suggested style, we changed the order of the sections, modified (decreased) the weight of TLS and have written clearer statements about the data capture. We have changed also the paper's title, although we kept the original slope stability analysis and FEM modelling. We think that our pilot site (the Sirok Castle) is just an example how these two nice tools can be combined in geological practice.

7) The method section needs to be improved adding more details about data acquisition and processing. Moreover, the authors often refer to the software used in the analysis. This is a good starting point, but it is important to specify the used criterion/procedure/equation. Please, separate the FEM global stability analysis from kinematic analysis or change the title of the section. In section 3.3, it is not clear: i) if the images were acquired using an image acquisition flight plan with a predefined frontal and side overlaps or in manual model, ii) if camera lenses were calibrated to reduce the effect of peripheral distortion that might affect/compromise the topographic reconstruction, iii) how image alignment was completed (e.g. automatic and keypoints based or picture centers coordinate based), iv) if/how the authors account for picture scale variation due to unconstrained relative elevation (in case of manual acquisition). In section 3.4, it is not clear if and how have you processed TLS point clouds for vegetation removal. Looking at figures 10a, 11a, 14a and 15a it seems that the vegetation was not removed. This compromise the topographic reconstruction of part of the slope creating local anomalies in morphological index maps.

Answer: The Materials and Methods section has been improved as the reviewer suggested. We have deleted many figures (equipment, as well as the duplications). The presented surface modelling is based on RPAS observations. More details (e.g. about flight control) is given about the processing of the imagery. There was no prior camera calibration, only simultaneous camera calibration, so this information was put into the text. GPS measurements were supported the georeferencing, which is documented in the section, too. Following the reviewer's suggestion, we have removed the TLS-oriented results to underline its validation role. With the deletion of TLS illustrations, the vegetation removal question is not relevant anymore.

8) In the Abstract the authors state that "joint system data were obtained from DTM and used as input parameters. . .". However, in section 3.7, the authors state that "main discontinuity sets were measured manually on site" and TLS and UAV (RPAS) models "had been used also to determine the most hazardous part of the hillslope for block stability analyses" since "many parts of the hillslope cannot have been measured manually". From these sentences, it is not clear how the TLS and UAV (RPAS) contributed to discontinuity measurement and how the authors process models for discontinuity extraction. Please clarify this aspect.

Answer: Joint system data was measured in the field and at inaccessible part the data set obtained by RPAS was also used for joint orientation. As we have clearly stated in the revised manuscript the main data capturing technology was based on an RPAS system. To be able to validate this dataset we performed TLS measurements. Both technologies were used to derive digital terrain (exactly surface) models (DSMs). After revising the paper, the TLS-based results were deleted and only the data quality check remained. The geological field measurements (i.e. all field works) were supported by the preliminary surface modelling results, so the manual inspections were “oriented” after the RPAS results.

9) In my opinion it is not clear which is the real contribution of morphological index maps to the study. If not supported by a specific description and comparison with field data the interpretation that the author made in the result section (i.e. “All resulting morphological maps strongly express the already eroded and potentially . . .”) might be only considered a speculation. The improvement of the description of the study area (see comment 4) might make easier the contextualization of these maps for the understanding of the ongoing slope evolution processes.

Answer: We have considered the reviewer’s opinion and have removed that part from the manuscript. One new figure (Fig. 7) shows the catchment area and the joint orientation obtained from the model. We would like to repeat our analysis a few years later after the first data capture to check the potential use of this technology to measure the volume and map the erosion. This is not part of the current paper.

10) The result of the stability analysis is not clearly described. Even if the author state that the critical global factor of safety is above 1, they then indicate that “the failure occurs in the weak layer” . . . In this way, it is not clear what the reader should conclude looking at the analysis. Probably they would state that the slope is stable in the modeled conditions but a perturbation might induce its failure with the formation of a slip surface that should nucleate from the weaker layer. Please clarify this aspect. Additionally, from the text it is not clear if the authors account for discontinuities in the global stability analysis.

Answer: The slope stability analysis was modified in the revised paper. A modified figure that shows the “weak layers” in the slope stability model is now part of the revised manuscript (new Fig. 8), clearly marking the calculated slip surface at the weak layers. A new figure that describes the studied sections is now part of the revised manuscript (Fig. 3). The difference between this model and the planar failure and wedge failure were described in more details. The revised text and Figs (Fig. 7) explains better the joint orientation and types of potential failures (planar and wedge failure).

11) The number, orientation and typology of the major discontinuity systems is not stated. The graph of figure 18 is not self-explanatory.

Answer: Former Figures 18 and 19 were removed and Fig 23-28 were compiled in 2 new figures showing the stereographic projection of the measured discontinuities and kinematic analyses of planar and wedge failures. Based on the projections six main joint sets (85/156, 88/312, 79/110, 81/089, 82/064, 61/299) are separated and given.

12) Consider to delete figures 2, 11, 12, 13, and 21. In my opinion they do not add particular value to the analysis. It is not clear which parts of the slope is shown in figures 9, 10, and 14. Please add a specific map. Indicate also the localization of the cross sections of figure 22. From the text, is not clear the number of tested sections and the width of the slope.

Answer: Fig. 2, Fig. 11, Fig. 12, Fig. 13 and Fig. 21 were deleted from the text. A new Figure was added (Fig 3) to show which parts of the slope are shown in new Figures and also mark the location of cross sections more clearly.

Out of 55 tested cross-sections 5 were chosen to calculate the global stability. The new Figure 8 shows two examples for the results of the analyses: Section 1 and 3 (see new Fig 3). Local stability analyses were not constrained to specified sections. Areas of the possible failures were determined with kinematic analyses.

13) The use of references is generally appropriate. Please, thoroughly check consistency of both citations in the text and list of references.

We have checked the references and citing in the text.

With the above corrections, I feel the manuscript may be reconsidered for publication.

Answer: We would like to thank to the anonymous reviewer for his/her valuable time spending with our manuscript and we do hope that the revision answer to the comments and suggestions of the reviewer.

Slope stability and rock fall hazard assessment of volcanic tuffs using ~~RPAS and TLS~~ with 2D FEM slope modelling

Ákos Török¹, Árpád Barsi², Gyula Bögöly¹, Tamás Lovas², Árpád Somogyi², and Péter Görög¹

¹Department of Engineering Geology and Geotechnics, Budapest University of Technology and Economics, Budapest, H-1111, Hungary

²Department of Photogrammetry and Geoinformatics, Budapest University of Technology and Economics, Budapest, H-1111, Hungary

Correspondence to: Ákos Török (torokakos@mail.bme.hu)

Abstract. Low strength rhyolite tuff forms steep, hardly accessible cliffs in NE Hungary. ~~A multi-dimensional approach including field analysis and laboratory tests was conducted to understand the mechanical properties of the tuff and to measure discontinuity surfaces. With the help of~~The slope is affected by rock falls. RPAS (Remotely Piloted Aircraft System) ~~and TLS (Terrestrial Laser Scanning) was used to generate~~ a digital terrain model (DTM) ~~was generated, and the results of these surveys were compared for slope stability analysis and rock fall hazard assessment.~~ Cross sections and joint system data ~~were~~was obtained from DTM ~~and used as input parameters for the slope stability analyses. The rocky slope, Joint and discontinuity system~~ was modelled also verified by field measurements. On site and laboratory tests provided additional engineering geological data for modelling. Stability of cliffs and rock fall hazard were assessed by 2D FEM (Finite Element Method) software and. Global analyses of cross-sections show that weak intercalating tuff layers may serve as potential hazards such as slip surfaces, however at present the highest hazard is related to planar failure, along ENE-WSW joints and to wedge failure and toppling were identified. The paper demonstrates ~~the usefulness of combined field analyses, geomechanical laboratory testing and various~~that without RPAS no reliable terrain model could be made and it also emphasizes the efficiency of RPAS in rock fall hazard assessment in comparison with other remote sensing techniques (such as RPAS and terrestrial laser scanning (TLS) in rock face stability calculations and failure mode analysis and tachymetry.

1 Introduction

~~Higher resolution geospatial data products have been developed at local, national, and global scale (Chen et al. 2016). Remotely piloted aerial systems can provide products that meet the requirements of national mapping (Cramer 2013), but also support applications such as coastal and glacial monitoring (Harwin and Lucieer 2012), monitoring of vegetation growth, military reconnaissance (Kostrzewa et al., 2003) and monitoring of forests (Rufino and Moeccia, 2005; Scholtz et al., 2011; Fritz et al. 2013) and of forest fires (Rufino and Moeccia 2005). These systems can be used in rapid mapping in emergency situations (Choi et al., 2009), in vegetation and/or biodiversity control but also enable the detection of several species such as orang-utans, elephants or rhinos and provide information on density and circulation of animals (Wich and Koh 2012), even counting birds (Grenzdörffer 2013). RPAS applications also cover the inspections of high and medium voltage lines, oil and gas pipelines, roads and railways (Colomina and Molina 2014), and can be used for data capturing of cultural heritage and archaeological sites (Rinaudo et al. 2012, Colomina and Molina 2014, Pajeres 2015).~~

In the past years, technological development of RPAS (~~Remotely Piloted Aircraft System~~) revolutionized the data gathering of landslide affected areas (Rau et al. 2011), recultivated mines (Haas et al. 2016), monitoring coastal processes (Casella et al. 2016), levee breaches (Brauneck et al. 2016) or road cuts (Mateos et al. 2016). ~~These tools have~~ RPAS has been increasingly used in engineering geology; historical landslide mapping (Jovančević et al. 2016) and in slope stability analyses (Niethammer et al. 2012) and in erosion process detection (Neugrig et al. 2016). ~~Another remote sensing method that has changed our understanding of landslide mechanism profoundly is,~~ Fraštia et al 2014.) RPAS can be combined with

terrestrial laser scanning (TLS) ~~which is a useful tool in failure analysis by providing slope geometries since both remote sensing tools provide high precision terrain measurement~~ (Fanti et al. ~~2012~~2013, Assali 2014, Francioni et al. 2014). The drawback of the latter method is that it is impossible to apply from the ground at hardly accessible cliff faces. Thus, it is much better to obtain a reliable Digital Terrain Model (DTM) and slope geometries with a combination of these tools. The application of these techniques brought significant amount of new data on previous landslides (Fanti et al. 2012, Neugrig et al. 2016) and also on failure forecast (~~(~~ Francioni et al. 2014, Neugrig et al. 2016, Manconi & Giordan 2015). ~~These tools can be used to validate height information derived by other technologies.~~ Rock falls represent special landslide hazards since their rapid movements and various trajectories make it difficult to predict their hazard potential (~~Costa~~Crosta & Agliardi 2003, Manconi & Giordan 2014). Several methods have been suggested to assess cliff stability from physical prediction rock fall hazard index (Crosta & Agliardi 2003) via Rockfall Hazard Rating System (Budetta 2004) and ~~to~~-modelling of their trajectories (Crosta & Agliardi 2002, Abbruzzese et al. 2009, Copons et al. 2009, Samodra et al. 2016). These methods rely on understanding failure mechanisms and on predicting displacement of rock masses (Pappalardo et al. 2014, Stead & Wolter 2015, Mateos et al. 2016) or at some cases individual rock blocks (Martino & Mazzanti 2014). To gather data on the rock fall hazard of existing cliff faces, a number of crucial data is needed: slope profiles, material properties, block size (De Biagi et al. 2017) and possible discontinuity surfaces that can contribute to slope instability. Slope profiles can be obtained ~~by TLS or RPAS from point clouds~~, while material properties have to be measured on site (e.g. UCS ~~Uniaxial Compressive Strength~~ by Schmidt hammer) or under laboratory conditions (Margottini et al. 2015). Detection and mapping of joints require fieldwork (on site measuring by compass), or at hardly accessible locations it is possible by applying remote sensing techniques (Fanti et al. ~~2012~~2013), or both.

Most of rock fall hazard publications deal with hard, well cemented rocks such as limestone (Samodra et al. 2016) or various other types of sedimentary rocks (Michoud et al. 2012), igneous or metamorphic rocks. In contrast, very few previous studies deal with cliff face stability and rock fall hazard of low strength rock such as volcanic tuffs (Fanti et al. ~~2012~~2013, Margottini et al. 2015). Volcanic tuffs are very porous rocks and prone to weathering (Arikan et al. 2007). While the current paper deals with a low strength pyroclastic rock, it has a slightly different approach of cliff stability analysis, since slope stability is assessed by using a combination of remote sensing techniques, field measurements, and laboratory testing of tuffs with 2D FEM (Finite Element Analysis) analyses of slopes. Compared to other case studies this study operates on a smaller scale and studies the possibilities of wedge and planar failures. The cliff face is unstable as it is evidenced by falling blocks. Due to rock fall hazard, the small touristic pathway was closed to avoid casualties. The current paper ~~analyzes~~analyses the cliff faces by condition assessment and stability calculations. Thus, this research provides an assessment of how ~~the combination of TLS with~~ RPAS can be used to create a surface model at hardly accessible sites. The paper also demonstrates the combined use of photogrammetric, surveying, and engineering geological methods at difficult ground conditions in assessing rock slope stability.

2 Study area

The study area is located at mid mountain range in NE-Hungary. A hardly accessible jointed rhyolite tuff cliff face was studied. On the top of the cliff a touristic point, the Sirok Castle is located (Fig. 1). The steep rhyolite tuff hill with an elevation of 298 m ~~AMSL~~ and found at the transition area of two mountain ranges, Mátra and Bükk Mountains. The tuff is very porous and prone to weathering (Török et al. 2007). ~~It shows similarities to the volcanic tuffs of Capadocia (Aydan et al. 2003).~~

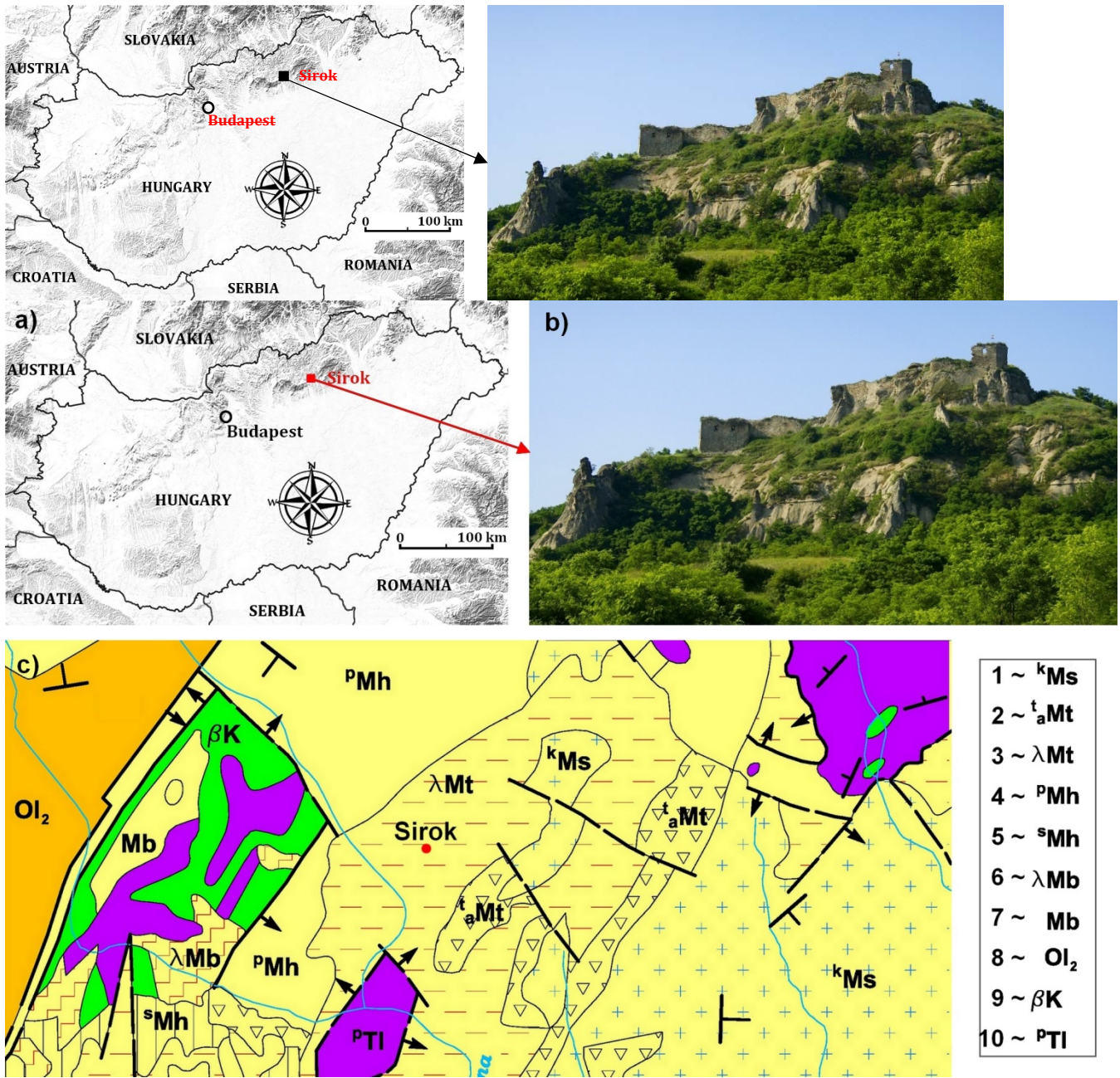


Fig.1. Location of studied cliff faces and an image of the rocky slope at Sirok Castle, NE Hungary (top) and the geological map of the area (redrawn after Balogh 1964) (bottom). Legend for geological map: Miocene (1-7), Oligocene (8), Cretaceous (9), Triassic (10): 1: gravel and conglomerate; 2: clay; 3: rhyolite tuff; 4: sand and sandstone; 5: siltstone; 6: rhyodacite tuff; 7: fine sand; 8: clay; 9: basalt; 10: radiolarite.

Although the first castle was already constructed in the 13th century AD, due to war damages and reconstructions, the current structure encompasses wall sections representing different construction periods. In these days, the partially ruined walls have been restored, and the castle is open to tourists but southern slopes are closed due to rock fall hazard.

The hill represents a rhyolite tuff that was formed during the Miocene volcanism (Badenian-Lower Pannonian period). The cliff face was formed during to the late Miocene volcanic activity. It is a part of the Inner Carpathian volcanic chain. The geological map of the closer area clearly reflects the dominance of pyroclastic rocks, with isolated occurrences of Oligocene and Triassic carbonates rocks (Fig. 21). The cliffs are steep and display several joints and discontinuity surfaces (Fig. 3). The present study focuses on the southern hillslope of the castle hill, where major rock falls occurred in the near past (Fig. 4-2). The study area is divided into smaller units, where RPAS and rock fall hazard assessment analyses were carried out (Fig 3).

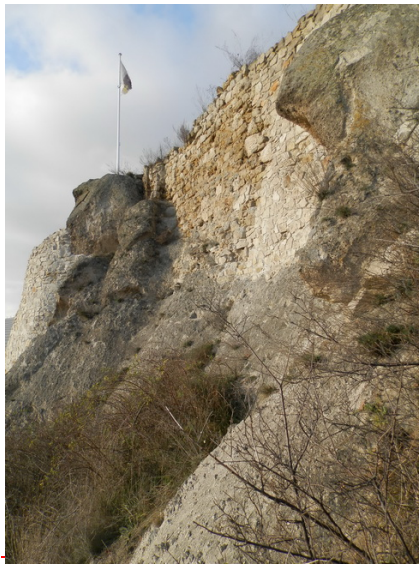


Fig.2. Steep cliff faces at Sirok Castle hill, southern slope

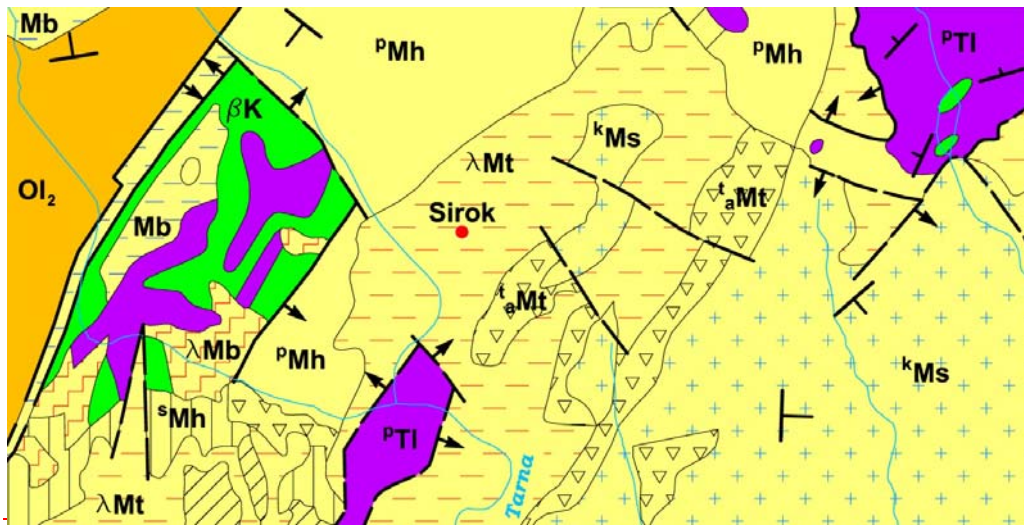




Fig.2. Fig.3. Geological map of the area (redrawn after Balogh 1964) Legend: Tl- Triassic carbonates, K- Cretaceous volcanic rocks, Ol- Oligocene sediments M- Miocene pyroclastic rocks

5



Figure.4. Studied southern cliff faces (clockwise): a) image of the castle obtained by RPAS with marked details; b) distant view of the eastern part of the cliff section; c) weathered rounded cliff with larger taffoni; d) vertical to sub-vertical cliff face with steep joints and traces of rock fall; e) steep cliffs dissected by joints.

10

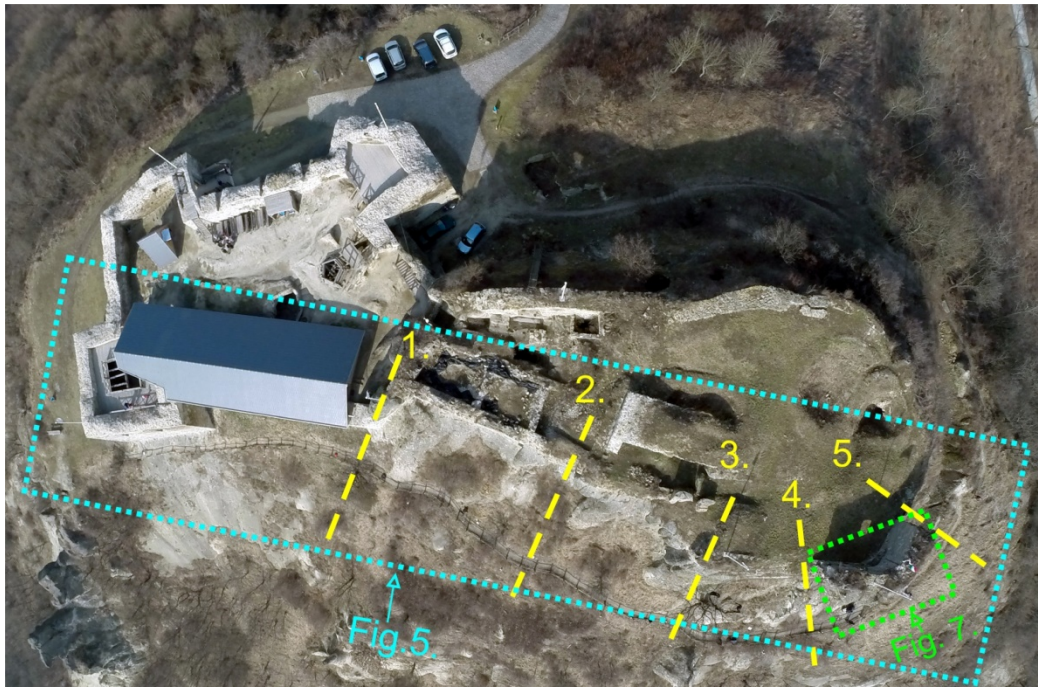
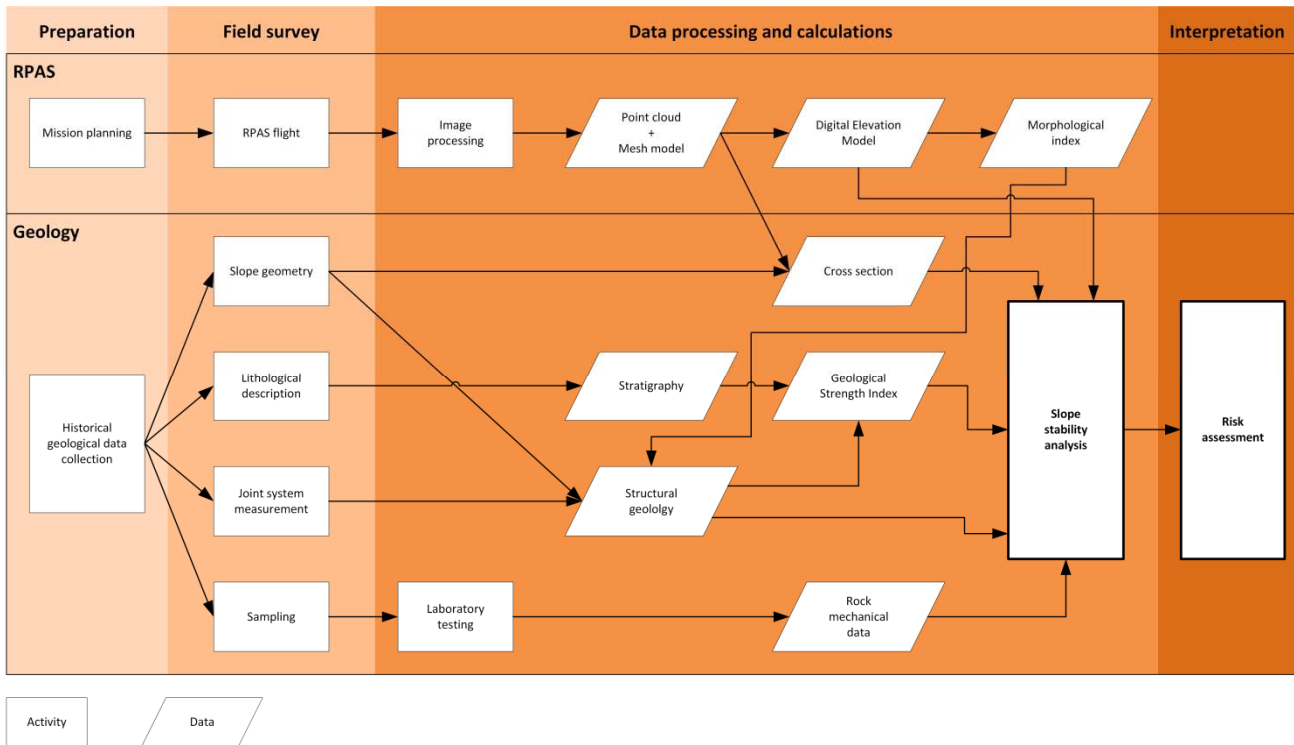


Fig.3. Location of the illustrations in the paper and the sections (1 to 5 marked by yellow dashed lines) where slope stability was calculated by using 2D FEM model (Fig.8). Dotted lines indicate the areas shown on Fig. 4 and Fig. 7.

3 Materials and Methods

5 The research contains two major methods: i) RPAS and ii) engineering geology. The applied methods are summarized in a flow diagram displaying the combination and links between (Fig. 4). The explanation of these research methods are given below in more details.



10 **Fig.4.** Flow chart showing the methods and obtained data set of this paper indicating the interrelationship between RPAS, geological analyses and risk assessment (see details in the text)

3.1 ~~Terrain~~RPAS data acquisition and terrain modelling

~~Cliff~~For cliff stability analysis a digital terrain model was required. It assumes the accurate 3D modelling of ~~thesethe~~ highly dissected rock faces. Since major parts of the site consist of hardly accessible steep slopes that are partly covered by vegetation, traditional surveying was not possible. As a consequence, ~~remote sensing technologies were applied. The first approach was to use only terrestrial laser scanning that allows rapid data acquisition and generation of 3D point clouds that—during post processing—allows creating surface models. Due to slope geometries and limited access to the cliff faces, oclusions, and disadvantageous incident angles, the detection of all slope geometries was not possible by using only TLS. Hence, additional terrain data was obtained by using two types of RPAS of slopes that surround the southern part of the castle (Fig. 5).~~RPAS technology was applied (Fig. 4). By the use of RPAS, high amount of images was captured, and then a 3D point cloud was generated to enable surface modelling. The point cloud was validated by terrestrial laser scanning, which is a mature, widely used technology in creating detailed, accurate surface models.



~~Figure 5. Applied remote sensing techniques (clockwise): Z+F Imager, 5010C DJI Phantom 2 with the GoPro Hero3+ action camera and Faro Focus S 120 3D~~

3.2 TLS

The terrestrial laser scanning (TLS) data were captured by two scanners, a Faro Focus S 120 3D (Faro, 2016) and a Z+F Imager 5010C (Z+F 2014). The terrestrial laser scanning was executed on 21st February 2015, when vegetation cover was limited and there was no snow cover. Although Faro scanner has less maximum measurement range than that of the Z+F (Table 1), it is a small, light scanner, easy to move and deploy, therefore this device was used on the top off the cliffs and on steep slopes. Both devices store all data on built-in memory cards.

Table 1: Technical parameter of the applied terrestrial laser scanners

| Scanner | Z+F Imager 5010C | Faro Focus S 3D 120 |
|---------------------------|--------------------|---------------------|
| Numbers of scan stations | 10 | 29 |
| Resolution | 3 mm/10 m | 3 mm/10 m |
| Ranging accuracy | 4 mm | 2 mm |
| Maximal measurement range | 187 m | 120 m |
| Scanning frequency | 1 016 000 points/s | 976 000 points/s |
| Scanning wavelength | 1500 nm | 905 nm |
| Color information | Yes | Yes |
| Tie points | Checkerboards | Spheres |

| | | |
|-----|------------------|--------------|
| Web | www.zf-laser.com | www.faro.com |
|-----|------------------|--------------|

Noticeably, the scanners were used with the same resolution in order to obtain near-equally dense point clouds. Similarly, both scanners have captured images to support identification during post-processing and to ensure providing enhanced quality end-products (Spreafico et al. 2015).

Because of the steep slopes and cliffs, the scanners could acquire point clouds in a limited range, so the cloud matchings get higher priority. The tie-objects were surveying markers, checkerboard plates of size A4, and spheres of diameter of 15 cm. During the entire time of the field work there were 38 tie-points marked by spheres and 7 further tie-points marked by checkerboards.

Due to georeferencing, particular tie-objects had to be measured also by Global Navigation Satellite System (GNSS). The used GNSS receiver was a Leica CS10 with a GS08plus antenna (GS08, 2014, CS10, 2014). The measurement was done in RTK mode supported by the Hungarian RTK network (RTKnet, 2013). There were 7 measured ground control points (GCPs); the mean 3D measurement accuracy was 4.9 cm (minimal value was 2 cm, maximal value 9 cm). The raw merged point cloud measured by Faro scanner contained 1.9 billion points, whilst the Z+F point cloud 0.8 billion points. After the resampling, these data-sets were reduced to 110 million and 40 million points, respectively. Both point clouds have X, Y-Z coordinates, intensity and RGB-color values (FaroScene, 2012, CC, 2014 Matlab, 2007, LeicaCyclone, 2016). The point cloud processing chain included several steps (Fig. 6).

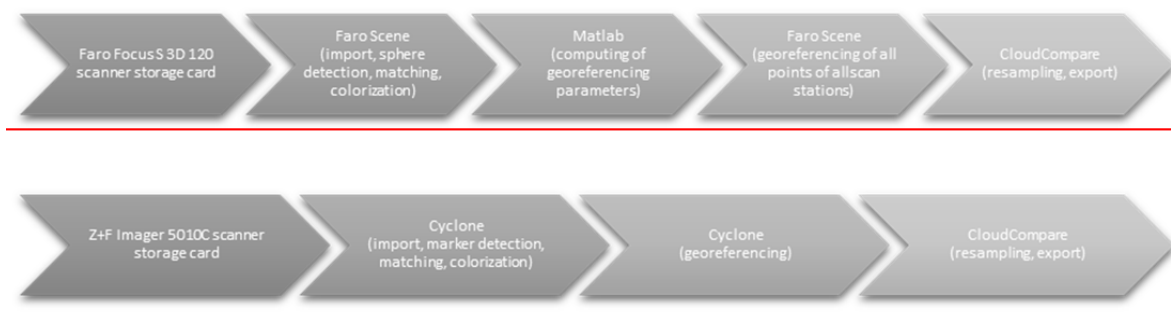


Figure 6. Processing of the terrestrial laser scanning data and the applied software environments

3.3 RPAS

The Remotely Piloted Aerial System (RPAS) (Eisenbeiss 2008) was deployed on the same day as the terrestrial laser scanning 21st February 2015, when vegetation cover was limited. The system is a modified commercial DJI Phantom 2 drone (DJI, 2016), where the flying vehicle has been equipped with a synchronous image transfer that also forwards the current flying parameters (e.g. height, speed, tilt, power reserve). Due to the complexity of the survey area, the flight was controlled manually; the required overlap between images was ensured by the operator considering capture frequency. For safety reasons, the crew consisted of two persons: one for controlling the aircraft, the other one for continuously monitoring the transferred video stream. The camera control is done by a tablet.

A GoPro Hero 3+ (GoPro, 2017) action camera was mounted onto a 2-DoF gimbal of the unmanned aerial vehicle (UAV). The camera has a fixed 2.77 mm focal length objective that is capable of capturing 4000 × 3000 pixel sized JPG images. The images were captured with a sensitivity of ISO 100 and sRGB color space. The lens was used with a fixed aperture of 2.8 and the camera was able to adjust the adequate shutter speed. Generally the exposure time was set to 1/1400 s and the images were compressed at a rate of 4.5 bits/pixel. There were three imaging flights; two around noon and one about 5 in the afternoon. The flying times were 13, 12 and 13 minutes, respectively, where 390, 365 and 419 images were captured. All

1174 images were involved in the photogrammetric object reconstruction (Fig. 75). The photogrammetric reconstruction has been done by Pix4Dmapper (Pix4D, 2017), which is based on Structure-from-Motion (SfM) technology (Westoby et al. 2012, Danzi et al. 2013, Lowe 2004). SfM automatically identifies tie points considering initial requirements (e.g. preliminary image centre positions, time stamps). Camera calibration was executed during post-processing, no prior calibration was needed. After the image alignment, the image projection centres and attitudes can be observed in (Fig. 84). 12 million points were obtained by the photogrammetric reconstruction.

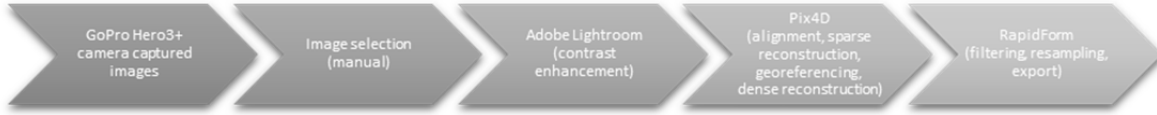


Figure 7. Processing of the RPAS collected imagery

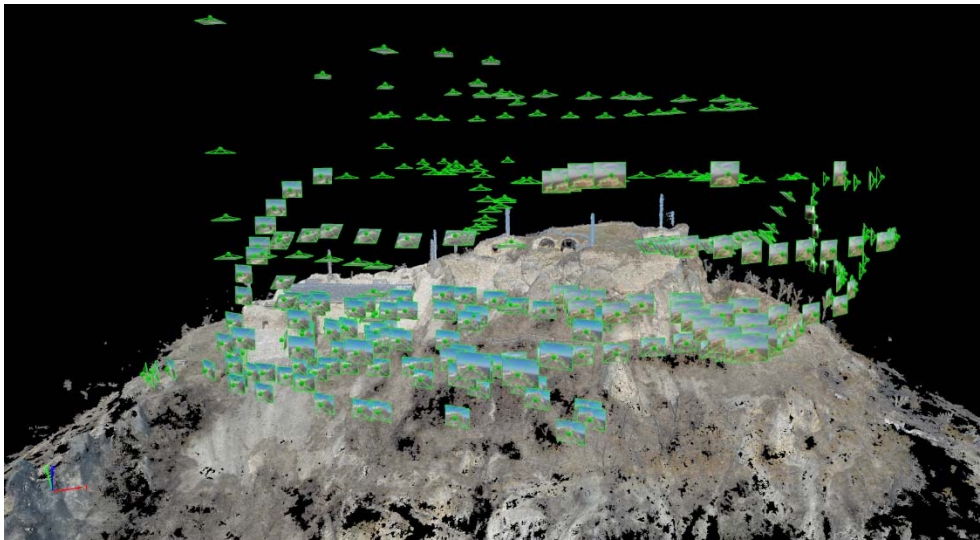


Figure 8

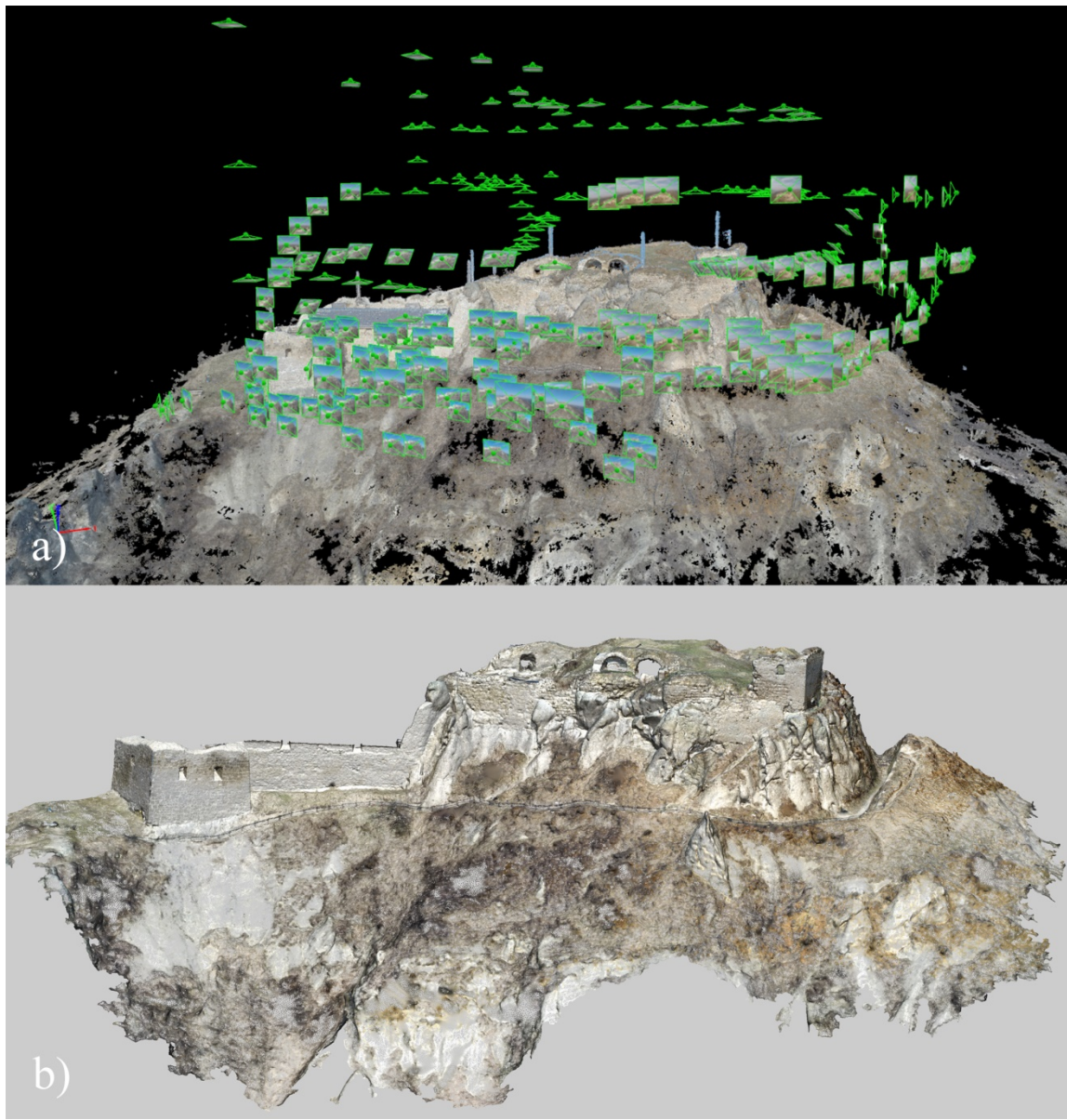


Fig.5. The captured image positions around the reconstructed castle hill (top) and the point clouds obtained by RPAS technology (bottom) (see top view on Fig. 3.)

Due to georeferencing, particular tie objects had to be measured also by Global Navigation Satellite System (GNSS). The used GNSS receiver was a Leica CS10 with a Gs08plus antenna (GS08, 2014, CS10, 2014). The measurement was done in RTK mode supported by the Hungarian RTK network (RTKnet, 2013). There were 7 measured ground control points (GCPs); the mean 3D measurement accuracy was 4.9 cm (minimal value was 2 cm, maximal value 9 cm).

3.4 Processing of raw point clouds, creating DEM and spatial analyses

The RPAS data collection was validated by the use of terrestrial laser scanning. The necessary data were captured by two scanners, a Faro Focus S 120 3D (Faro, 2016) and a Z+F Imager 5010C (Z+F 2014). The terrestrial laser scanning was executed on the same day as the RPAS mission. The raw point cloud measured by Faro scanner contained 1.9 billion points, whilst the Z+F point cloud 0.8 billion points. Both point clouds have X, Y Z coordinates, intensity and RGB color values. RPAS and TLS based point clouds could be compared by the software CloudCompare (CloudCompare, 2014) (Fig. 4).

The RPAS technology has produced considerable amount of points—obtained is multiplications of the surface points. The redundancy is because of the doubled terrestrial laser scanning and of the UAV survey. Since the merged this point cloud is difficult to be managed due to its size, and has heterogeneous point spacing, the later processing requires the elimination of the redundancy. First, each point cloud was resampled a sophisticated resampling step, which was done by CloudCompare, where the spatial resolution of the point clouds was set to 1 cm. After this reduction, the laser scanned point clouds were merged and resampled to 1 cm spatial resolution.

The laser scanned point clouds were then imported into Geomagic Studio 2013 (GeomagicStudio, 2013) and the mesh model with 1 cm triangle side lengths was derived. The UAV point cloud was also imported and meshed, but where the triangle side length was 5-7 cm.

(Fig. 7). To support the geological survey, several horizontal and vertical sections (Fig. 9) were derived in Geomagic DesignX 2016 (GeomagicDesignX, 2016); these profiles were exported in CAD-format (DXF Fig. 5).

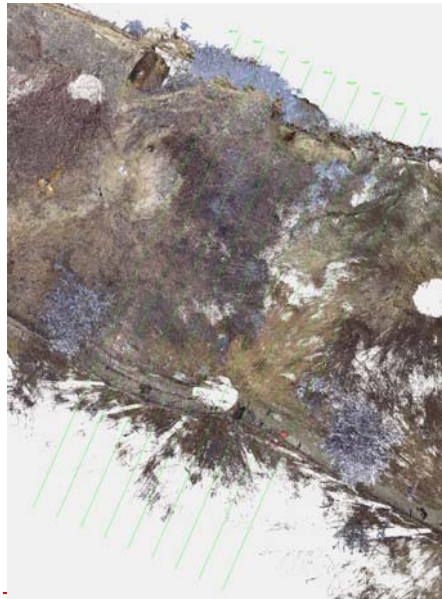


Figure 9. Vertical sections marked by parallel green lines to support geologic analyses

The next step was to make cut-offs focusing only on the cliffs; it was done by CloudCompare, followed by the TLS and UAV points being exported in LAS-format (LAS, 2012). The exported points could then be imported into SAGA GIS 2.1.2 (Conrad et al. 2015), where the necessary DEMs were created by inverse distance weighting (IDW) algorithm (IDW, 2013). The derived DEM-grids have 5 cm spatial resolution, which is adequate for morphologic analyses (Fig. 4). The morphology analysis has concentrated on Catchment Area (CA), Stream Power Index (SPI) and (Haas et al. 2016), although several other morphological indices (e.g. Topographic Wetness Index (TWI) (Haas et al. 2016, Stream Power Index) were derived (Fig. 4). These indices express the potential relationship between surface geometry and geological parameters.

The visualization is further supported by developing Streetview-like demonstration environment; a dedicated web site is designed, where the users have an access of the surface image as well as the necessary navigation tools (move forward, backward, rotate and zoom). This solution has less importance in hazard evaluation but it gives the possibility to look around and check what is visible near the rocks.

3.52 Engineering geological field measurements geology and slope stability analysis

Field data collection formed the first part of engineering geological surveys. Major lithotypes were identified and described and geological profiles were recorded during the engineering geological field surveys (Fig. 4). Rock joints, discontinuity surfaces and fault systems were measured by using compass and structural geological software applied in mobile phone. The structural geological data was analyzed by Dips software. Strength parameters were assessed on site by using a

Schmidt hammer. 10 rebound values were measured on each surface and mean values and standard deviations were also calculated. This method has been also used previously to gather rapid data on rock strength of cliff faces (Margottini et al. 2015). The data-set was compared to rock mechanical laboratory tests.

3.6 Rock mechanical laboratory tests

Samples for laboratory analyses were collected on site- (Fig. 4). Major rock mechanical parameters were measured under laboratory conditions on cylindrical specimens. These were drilled from blocks and cut into by appropriate size using cutting disc. The sizes of tested specimen were made according to EN on air dry and on water saturated samples. The specimens were grouped according to the bulk density and the propagation speed of the ultrasonic pulse wave. Strength parameters such as uniaxial compressive strength, an indirect tensile strength (Brazilian), was measured according to relevant EN standards and ISRM suggested methods and modulus of elasticity was also calculated (Table 21). The generalized Hoek-Brown failure criterion (Hoek et al. 2002) was used to determine strength parameters of the rock mass. Altogether, 53 cylindrical test specimens were used for the tests.

Table 21. Rock mechanical tests and relevant standards.

| Rock mechanical parameter | Number of specimens | Relevant standard |
|--|---------------------|-----------------------------------|
| Bulk density | 53 | EN 1936:2000 |
| Water absorption | 18 | EN 13755:2008 |
| Propagation speed of the ultrasonic wave | 53 | EN 14579:2005 |
| Uniaxial compressive strength | 31 | EN 1926:2006 ISRM 2015 |
| Modulus of elasticity | 31 | ISRM 2015 |
| Tensile strength (Brazilian) | 23 | ISRM 2015 |

3.7. 2D FEM modelling

~~The stability analysis of the rocky slopes was focused on the southern slopes. The falling blocks can endanger the touristic footpath bellow the castle. The FEM modelling was made on the southern slopes, therefore the stability analysis of the rocky slopes was focused on this part of the cliff (Fig. 3). First, the rock mass failure was analysed with by the RocFall FEM software of the Rocscience- (RS2). The steepest sections were determined from to the terrain model obtained from RPAS data. The GSI values of the rock masses were determined according to Marinós et al. (2005). The rock slope global stability of the investigated hillslope of selected sections was analyzed according to Hudson & Harrison (1997)-calculated with RS2 software. Since the rhyolite tuff is a weak rock with few joints the rock mass failure and the failure along discontinuities were also analysed. This kinematic analysis had been done with stereographic tool. The orientations of main joint sets were obtained from RPAS (DTM model, Fig. 4) and at accessible areas were also measured on site on the southern and south-eastern parts of the hillslope. Additional measurements were also made in the underground cellar system of the castle, where the tuff is also exposed. The Dips software was used for the kinematic analysis. The direction of the hillslopes and the direction of the discontinuities were compared to determine the location of the potential hazardous failure zones on the hillside. analyzed. Kasmer et al. (2013) used FEM software for stability analysis of Cappadocian tuffs. Shakhmekhi & Tannant (2015) used FEM software for probabilistic rock. Stereographic plots were generated showing the possible failure planes for all slope directions and the safety factor of the possible planar failure was calculated by Rocplane software. Wedge failure was modelled by Swedge software. Toppling failure due to geological and geomorphological conditions~~

cannot occur. Risk assessment was based on slope stability analysis considering the variability of joint geometry calculations (Fig. 4).

4. Results

The rhyolite tuff faces consist of moderately bedded ignimbritic horizons and also brecciated lapilli tuffs and tuffs according to our field observations (Fig. 6). The topmost 10 metres of the cliff face which was modelled from slope stability comprises 3 main horizons and can be modelled as “sandwich structure”. The lower and the upper part are formed by thick pumice containing lapilli tuffs. These beds enclose nearly 2 metres of well-bedded less-welded fine tuff and brecciated horizons (Fig. 6).

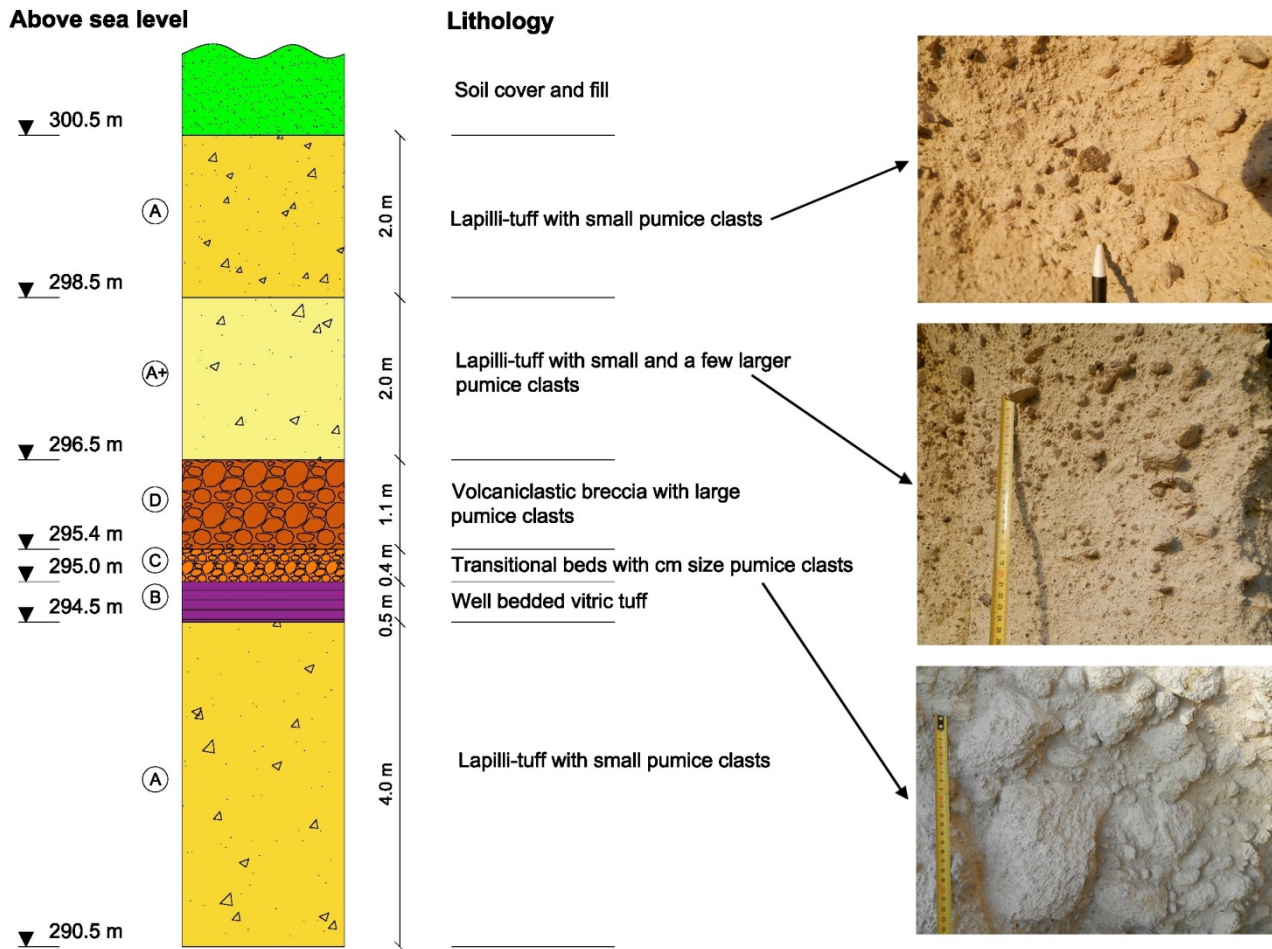


Fig.6. Lithologic column of Sirok Várhegy showing the modelled topmost 10 metres section of the hill (letters refer to lithologic units)

Combining and comparing all measured data of discontinuities and joints, using DTM and morphological index (Fig. 4) the structural geological conditions were clarified: six main joint sets (85/156, 88/312, 79/110, 81/089, 82/064, 61/299) were identified with prevailing NE – SW direction (Fig. 7).

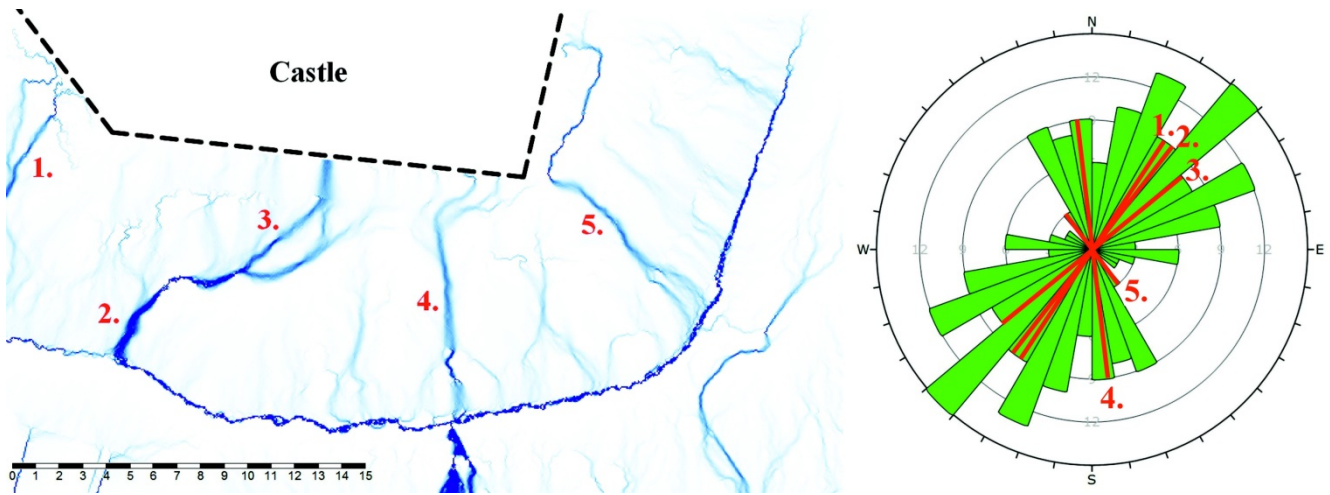


Fig.7. Top view of the cliff (see the location on Fig. 3) obtained with RPAS and the catchment area diagram obtained from DEM analysis (Fig. 4) that was used for joint pattern recognition. Numbers refer to major joint systems marked on DEM map and on rose diagram of the field measurements and RPAS data set.

The laboratory tests of tuffs provided the input data for stability analysis for the two main lithologies: upper and lower unit of lapilli tuff and middle unit of less welded tuff (Table 2). In the model calculations GSI=50 value was used.

Table 2. Rock mechanical parameters of tuff used in the model: lapilli tuff refers to upper and lower 4 metres, less welded tuff refers to middle stratigraphic unit

| | <u>Upper and Lower unit</u> <u>(marked by A on Fig. 10)</u> <u>(Lapilli tuff)</u> | <u>Middle unit</u> <u>(marked by B-D on Fig. 10)</u> <u>(Less welded tuff)</u> |
|----------------------------|---|--|
| <u>Mechanical property</u> | | |

| | | | |
|---|---------------------------|-------------|-------------|
| <u>Bulk density(ρ)</u> | <u>[kg/m³]</u> | <u>1815</u> | <u>1635</u> |
| <u>Uniaxial compressive strength(σ_c)</u> | <u>[MPa]</u> | <u>8.02</u> | <u>0.35</u> |
| <u>Tensile strength (σ_t)</u> | <u>[MPa]</u> | <u>0.83</u> | <u>0.04</u> |
| <u>Modulus of elasticity(E)</u> | <u>[GPa]</u> | <u>0.97</u> | <u>0.05</u> |

The results of RS2 FEM analyses suggest that the global factor of safety is SRF=1.27-1.71 in the studied sections (see some of the selected sections are shown on Fig 4). The SRF factor is influenced by the weak tuff layer (Fig. 6) which has very low shear strength compared to the lapilli tuff. Our failure analyses have demonstrated that the bottom of the slip surface would be in the weaker layer (marked by B-D on Fig. 8) and could lead to a larger mass movement.

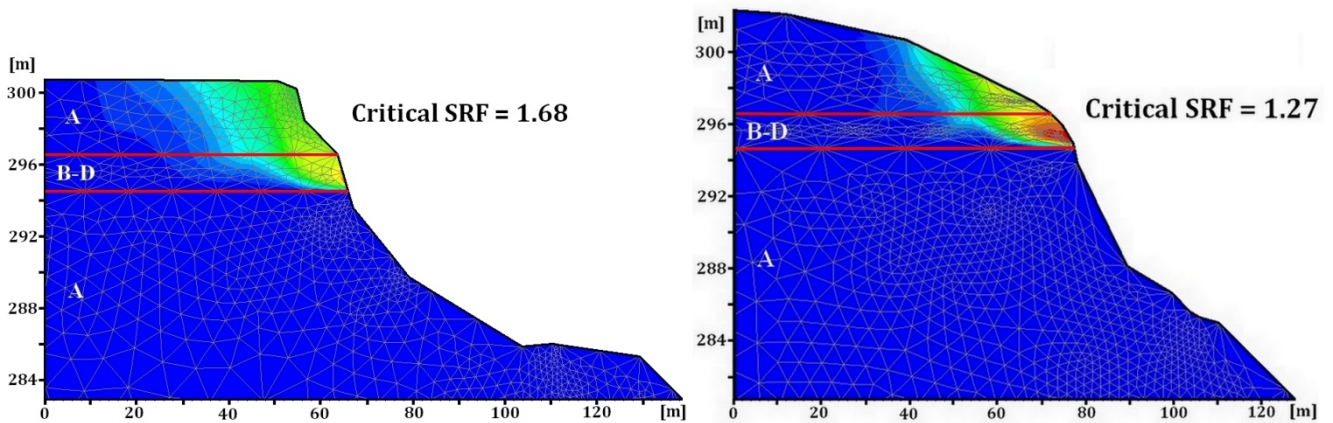


Fig.8. The results of the global stability analysis of the slopes (sections 3 and 4 on Fig. 3), total displacements are marked in blue to red (lithology is indicated by letters A-D, note the weak zone marked by B-D, description of lithologies is given on Fig.6.)

Other failure modes that were studied are planar failure and wedge failure, which are often controlled by joints and discontinuities. According to DTM joint analyses (Fig. 7) and field recordings there was no regular spacing of the discontinuities. Stereographic plots with possible failure planes for all slope directions (Fig. 9) indicate that the most hazardous part of the slope is the one where the plane orientation is 75/75. The calculated factor of safety (FS= 1.15) implies high probability of planar failure.

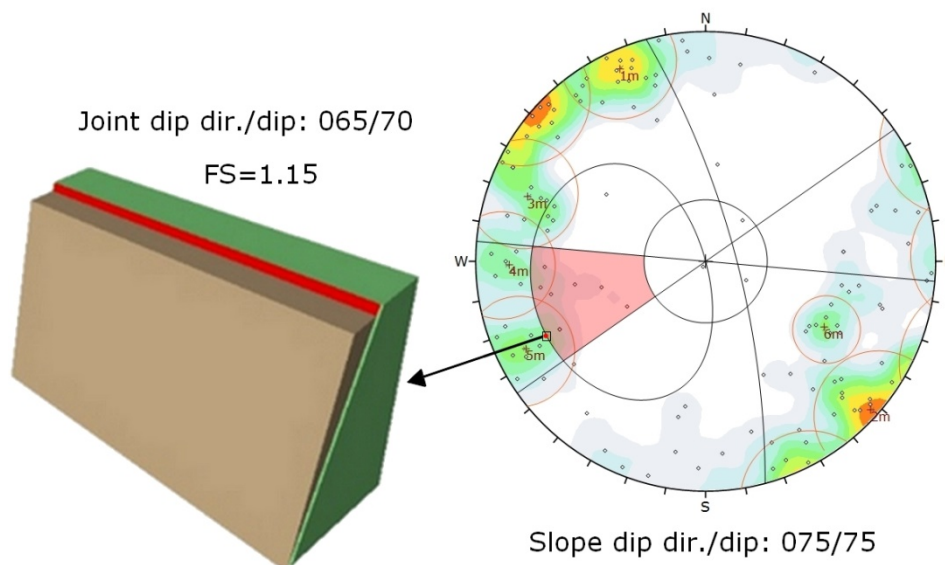


Fig.9. Kinematic analysis of planar failure by Rockplane

Three possible wedge failure modes were identified as being the most hazardous, according to our calculations by Swedge software (Fig. 10). In these three cases the factor of safety was in the range of 1.38-1.94 representing the hazards of rock falls along wedges delineated by different joint systems.

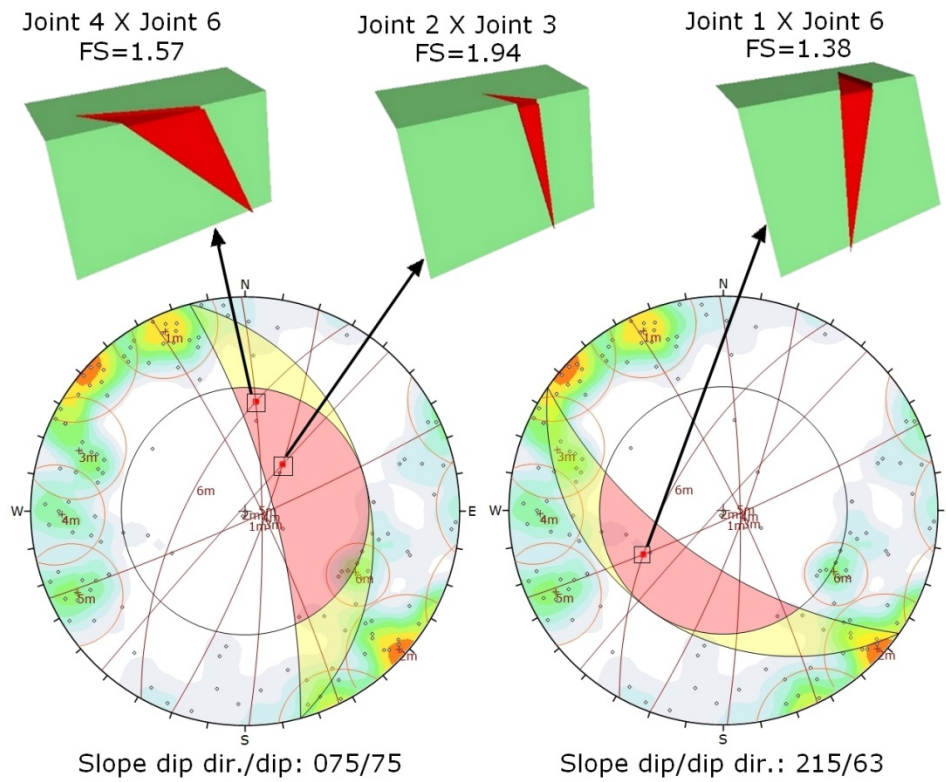


Fig.10. Examples for the kinematic analysis of wedge failures

5. Discussion

There are three critical sets of input data in modelling of rocky slopes: i) terrain model and slope geometry, ii) joints system and iii) strength of rock mass.

To obtain the first, the slope geometry, RPAS based surveying technique was used, because even the hardly accessible cliffs could be surveyed with this method (Giordan et al. 2015). First, the rock-mass failure was analyzed with RS2 FEM software on the steepest sections which was determined according to the TLS and UAV model. Muceku et al. (2016) show a complex slope stability analysis of a heritage town with the same FEM software.

Secondly, the kinematic analysis had been done with stereographical tool. The planes of the main discontinuity sets were measured manually on site. Many parts of the hillslope cannot have been measured manually, therefore, the TLS and UAV model had been used also to determine the most hazardous part of the hillslope for block stability analyses. Nowadays TLS and UAV measurements are commonly used for rock slope stability analysis. Aliardi et al. (2013) used TLS measurements for investigation of structurally controlled instability mechanism. Tuckey & Stead (2016) investigated the determination of the two critical factors of rock slope instability: the persistence of discontinuities and intact rock bridges with remote sensing methods. Liu et al. (2017) used digital photogrammetry tools to determine the geometrical characteristic of discontinuities

for block stability analysis. During the kinematic analysis planar sliding, wedge sliding, and toppling failure were tested with Dips software. Probabilistic kinematic analysis had been done with grid based GIS method, as in Park et al. 2015, in order to map the dangerous zones of the rock slopes of a road. The determination of the safety factor of the dangerous blocks was made by LEM analysis with Rocscience software.

4. Results and discussion

4.1. Comparison of RPAS and TLS data

The two, basically different data collection techniques resulted in RPAS based data had to be validated. TLS measurements were used for this, in a way that the two point clouds covering the surface. These clouds were resampled, so their in order to homogenize the spatial resolution was homogenized. These two models are suitable to compare the data collection techniques (Fig. 10).

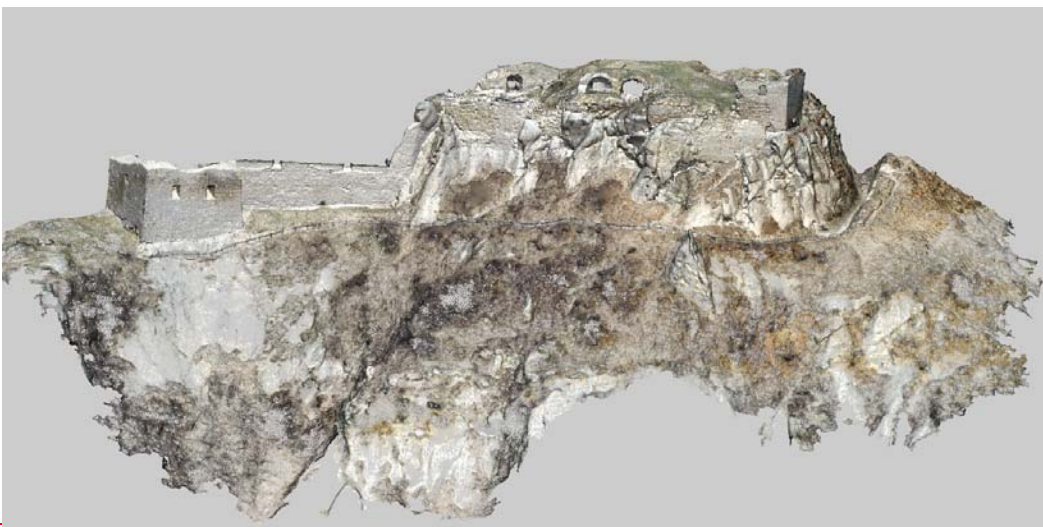


Figure 10. The point clouds obtained by TLS (top) and by RPAS (bottom) technologies

The raw point clouds were transferred into geographic information system, where the digital elevation models were created (Fig. 11).

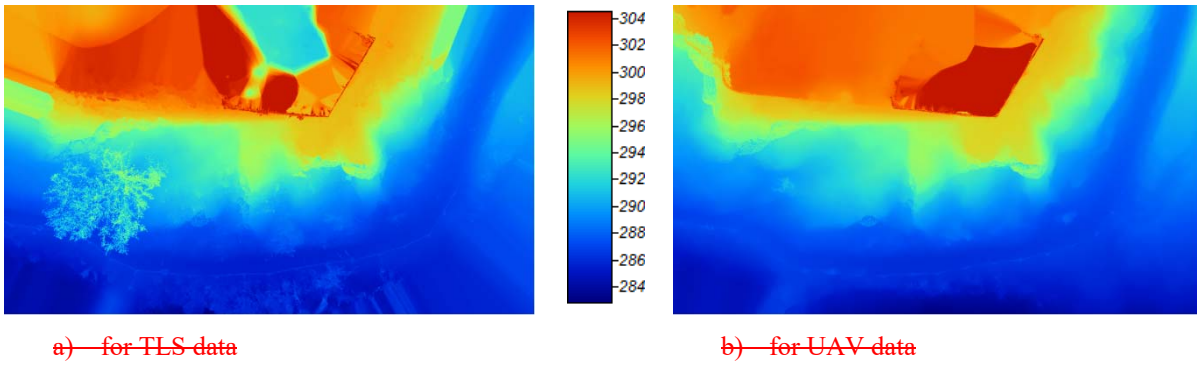


Figure 11. The Digital Elevation Models

5

First, the point density is densities have been tested; in CloudCompare, as a unit sphere of volume of 1 m³ was defined where the points can be counted and then the sphere can be moved along the whole surface. The point amounts in the unit spheres represent the data collection density (Fig. 12. and Fig. 13).

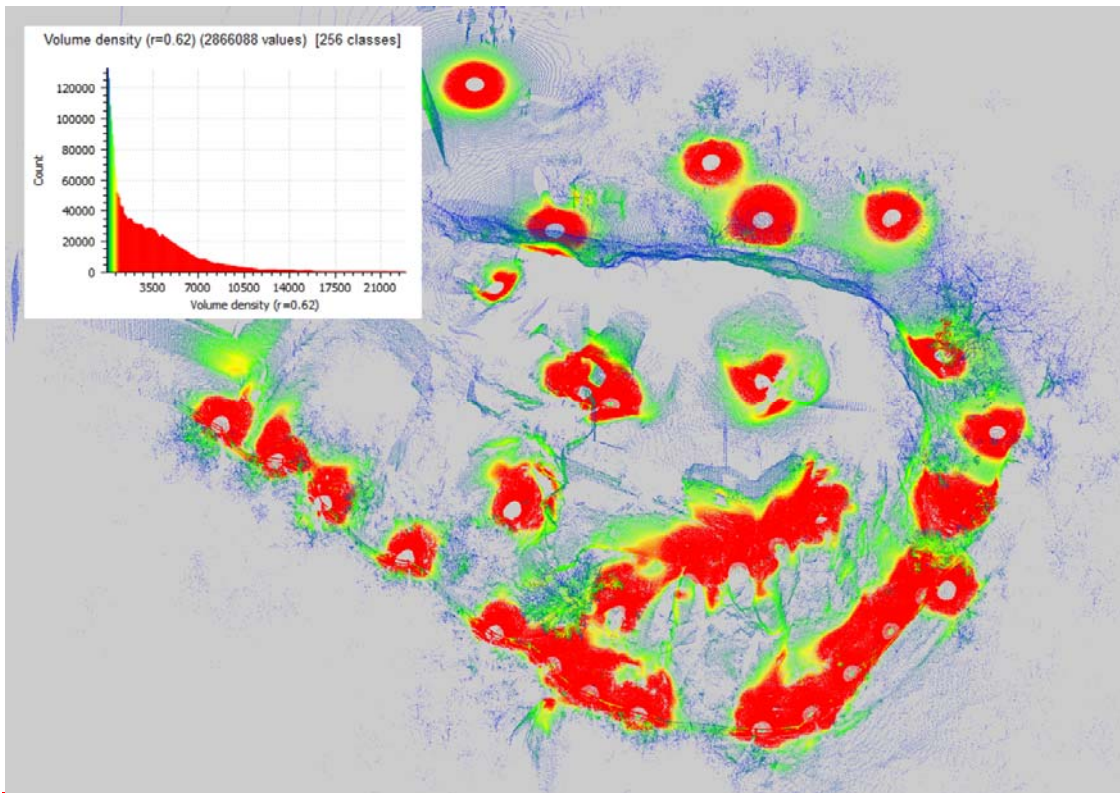


Figure 12. TLS point cloud densities derived by the use of a 1 m³-unit sphere

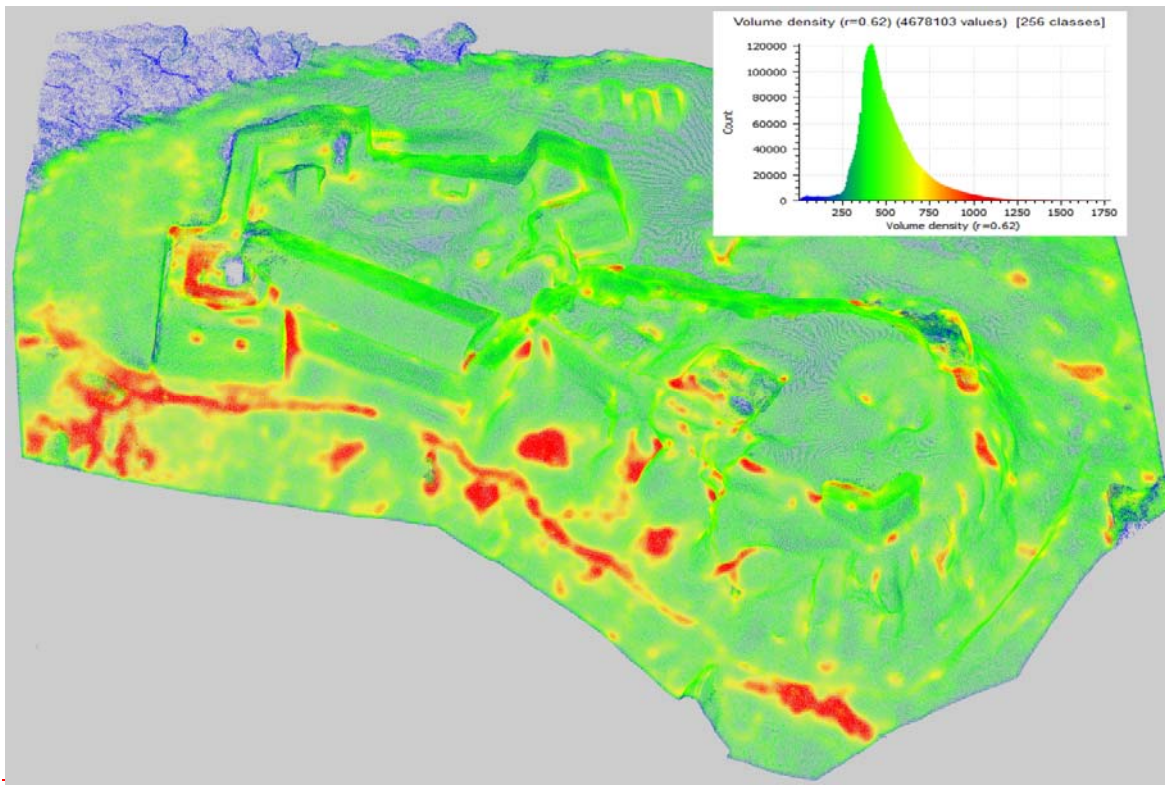


Figure 13. UAV point cloud densities derived by the use of a 1 m³-unit sphere

Obviously, the terrestrial laser scanning dataset has significantly higher point densities. This computation proved that the average point density in both point clouds are practically the same, although the RPAS densities are more homogeneous, while the TLS has denser point clouds close to the scanning stations, which is indicated in the figure by the red clusters (Fig. 12). The UAV data is much more homogeneous; it is because of the less original data density.

Another aspect causing some differences between the two data sets is that the image based reconstruction is performed by interest operators, very usually SIFT (Scale-invariant Feature Transform) or similar computer vision operators (Lowe 2004). These operators are generally sensitive to intensity jumps, points, or corners, and textural changes in the input images. If the image resolution is not adequate or the object is locally “smooth”, these operators do not return with surface points and the output of the reconstruction has some “filtered” effect. This phenomenon is clearly visible on the cliffs; the smoothing effect can excellently be seen by the Analytical Hillshading (AH) (Fig. 14). Fortunately, the surface reconstruction quality in RPAS processing resulted minor, ignorable smoothing effect. Comparing the two data sets, it is clearly proven that the geometric resolution of the RPAS-based digital elevation model corresponds to the TLS one, offering the same quality level as the terrestrial laser scanning.

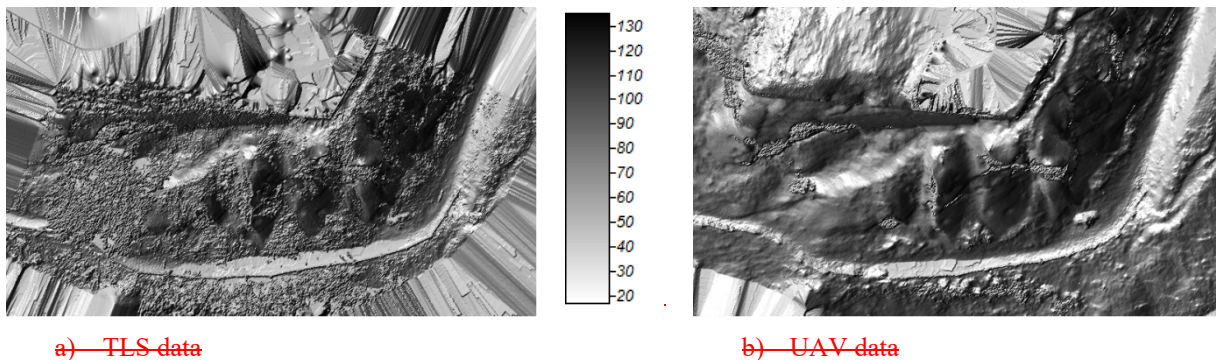


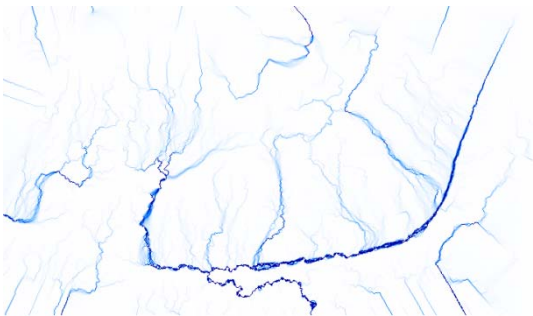
Figure 14. Analytical hillshading as surface smoothness representation

The digital elevation model can be analyzed in terrain morphological sense. The Catchment Area (CA), Stream Power Index (SPI) and the Topographic Wetness Index (TWI) derived for both data sets is shown in Fig. 15 to be compared to the UAV image of the same area. All resulting morphological maps strongly express the already eroded and potentially unstable 'prone to erosion' parts of the cliff. Compared the two data sets, it is clearly proven that the geometric resolution of the UAV based digital elevation model corresponds to the TLS one, so the faster, simpler, and cheaper UAV based surveying technology offers similar quality results as the terrestrial laser scanning (Fig. 14).

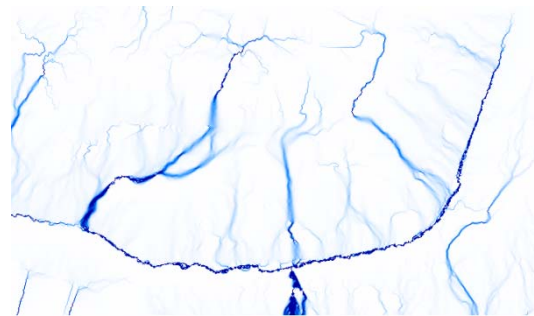
5



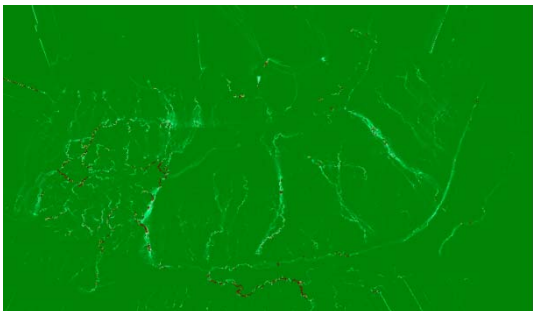
a) UAV captured image



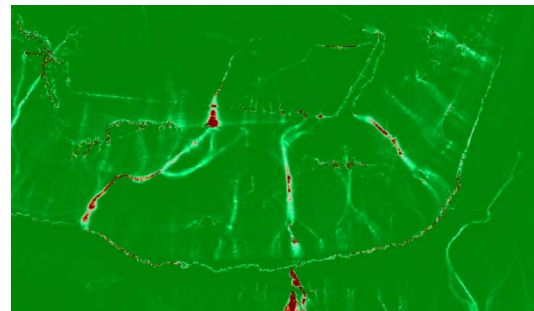
b) Catchment area for TLS DEM



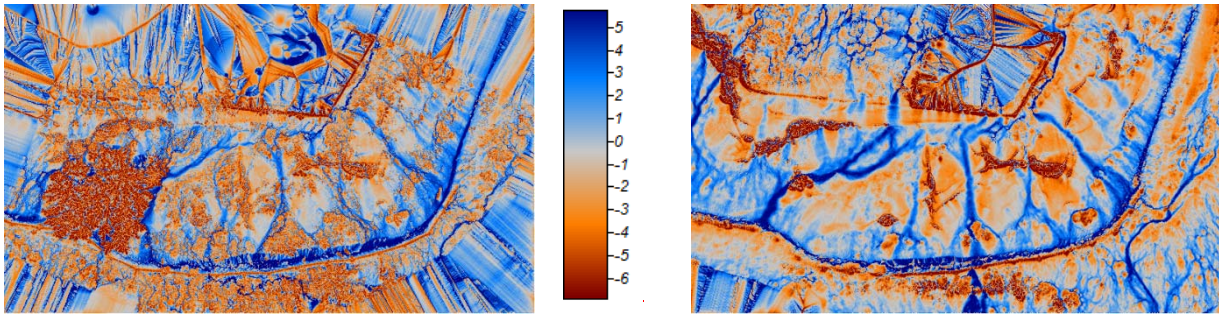
e) Catchment area for UAV DEM



d) Stream Power Index for TLS DEM



e) Stream Power Index for UAV DEM



f) Topographic Wetness Index for TLS
DEM

g) Topographic Wetness Index for UAV
DEM

Figure 15. Cliff and the corresponding morphological results for TLS and UAV data sets

4.2. Compilation of engineering geological field and laboratory data

The rhyolite tuff faces consist of moderately bedded ignimbritic horizons and also brecciated lapilli tuffs and tuffs according to our field observations (Fig. 16). The topmost 10 metres of the cliff face which was modelled from slope stability comprises 3 main horizons and can be modelled as “sandwich structure”. The lower and the upper part are formed by thick pumice containing lapilli tuffs. These beds enclose nearly 2 metres of well bedded less welded fine tuff and brecciated horizons (Fig. 17).



Figure 16. Lapilli tuff the dominant lithology of the studied cliff

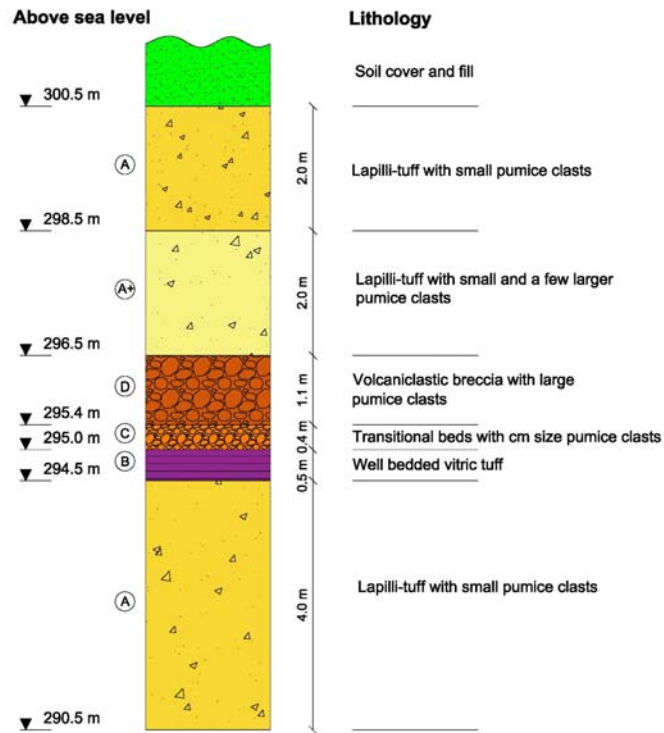


Figure 17. Lithologic column of Sirok Várhegy showing the modeled topmost 10 metres section of the hill

The orientation of discontinuities and joints was measured on the S and SE part of the hillslope. Discontinuities which are close to the footpath were measured manually while the hardly accessible ones were identified on images obtained by TLS and UAV (Fig. 18).

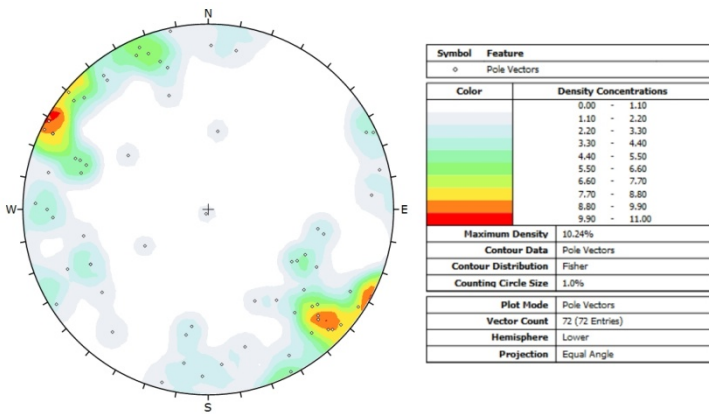


Fig. 18. Stereographic plot of the discontinuities on the southern part of the hill

~~Additional measurements were also made in the underground cellar system of the castle, where the tuff is also exposed. These identified discontinuities were also documented by TLS (Fig 19). Combining and comparing all measured data of discontinuities and joints a prevailing NE—SW on the southern hillside (Fig. 20).~~

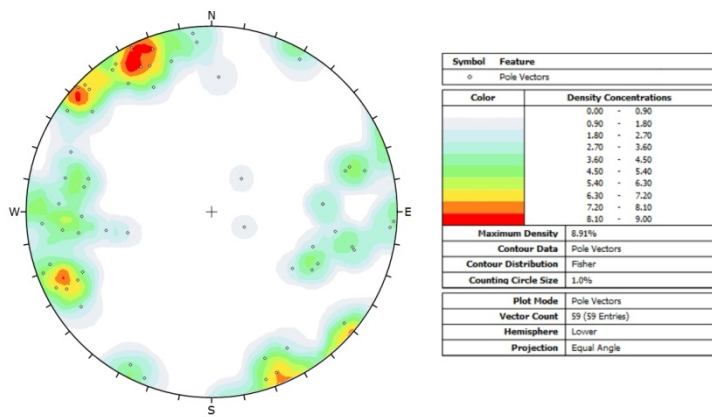


Figure 19. Stereographic plot of the discontinuities measured in the cellars

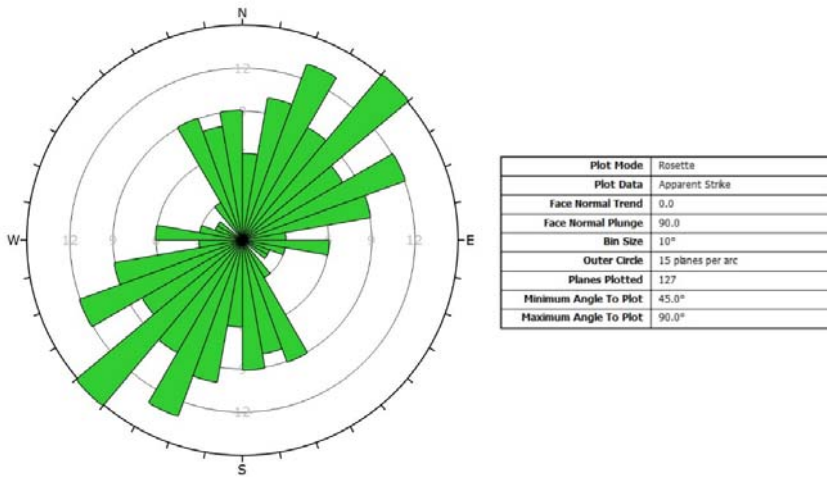


Figure 20. The frequency of joints measured on the castle hill

5 The laboratory tests of tuffs provided the input data for stability analysis for the two main lithologies: upper and lower unit of lapilli tuff and middle unit of less welded tuff (Table 3).

The GSI values were determined according to Marinos et al. (2005). In the model calculations GSI=50 value was used (Fig. 21).





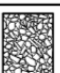

| GEOLOGICAL STRENGTH INDEX FOR JOINTED ROCKS (Hoek and Marinos, 2000) | | SURFACE CONDITIONS | | | | |
|--|--|---|--|---|--|--|
| <p>From the lithology, structure and surface conditions of the discontinuities, estimate the average value of GSI. Do not try to be too precise. Quoting a range from 33 to 37 is more realistic than stating that GSI = 35. Note that the table does not apply to structurally controlled failures. Where weak planar structural planes are present in an unfavourable orientation with respect to the excavation face, these will dominate the rock mass behaviour. The shear strength of surfaces in rocks that are prone to deterioration as a result of changes in moisture content will be reduced if water is present. When working with rocks in the fair to very poor categories, a shift to the right may be made for wet conditions. Water pressure is dealt with by effective stress analysis.</p> | | SURFACE CONDITIONS | | | | |
| | | VERY GOOD Very rough, fresh unweathered surfaces | GOOD Rough, slightly weathered, iron stained surfaces | FAIR Smooth, moderately weathered and altered surfaces | POOR Slickensided, highly weathered surfaces with compact coatings or fillings or angular fragments | VERY POOR Slickensided, highly weathered surfaces with soft clay coatings or fillings |
| STRUCTURE | | DECREASING SURFACE QUALITY → | | | | |
|  | INTACT OR MASSIVE - intact rock specimens or massive in situ rock with few widely spaced discontinuities | 90 | 80 | 70 | N/A | N/A |
|  | BLOCKY - well interlocked undisturbed rock mass consisting of cubical blocks formed by three intersecting discontinuity sets | 80 | 70 | 60 | | |
|  | VERY BLOCKY - interlocked, partially disturbed mass with multi-faceted angular blocks formed by 4 or more joint sets | 70 | 60 | 50 | | |
|  | BLOCKY/DISTURBED/SEAMY - folded with angular blocks formed by many intersecting discontinuity sets. Persistence of bedding planes or schistosity | 60 | 50 | 40 | | |
|  | DISINTEGRATED - poorly interlocked, heavily broken rock mass with mixture of angular and rounded rock pieces | 50 | 40 | 30 | | |
|  | LAMINATED/SHEARED - Lack of blockiness due to close spacing of weak schistosity or shear planes | N/A | N/A | 20 | | 10 |
| | | ↑ DECREASING INTERLOCKING OF ROCK PIECES | | | | |

Figure 21. GSI of moderately jointed rock mass of castle hill (GSI=50, see red circle) (table is from Marinos et al. 2005)

Table 3. Rock mechanical parameters of tuff used in the model: lapilli tuff refers to upper and lower 4 metres, less welded tuff refers to middle stratigraphic unit

| Mechanical property | | Upper and Lower unit (Lapilli tuff) | Middle unit (Less welded tuff) |
|---|----------------------|--|-----------------------------------|
| Bulk density(ρ) | [kg/m ³] | 1815 | 1635 |
| Uniaxial compressive strength(σ_c) | [MPa] | 8.02 | 0.35 |
| Tensile strength(σ_t) | [MPa] | 0.83 | 0.04 |
| Modulus of elasticity(E) | [GPa] | 0.97 | 0.05 |

4.4. Slope stability modelling

The global stability of the hillslope was calculated by using RS2 FEM software. The results suggest that the global factor of safety is SRF=1.27-1.71. The SRF factor is influenced by the weak tuff layer which has very low shear strength compared to the lapilli tuff. Our failure analyses have demonstrated that the bottom of the slip surface would be in the weaker layer (Fig-22). These results indicate that failure occurs in the weak layer and could lead to a larger mass movement.

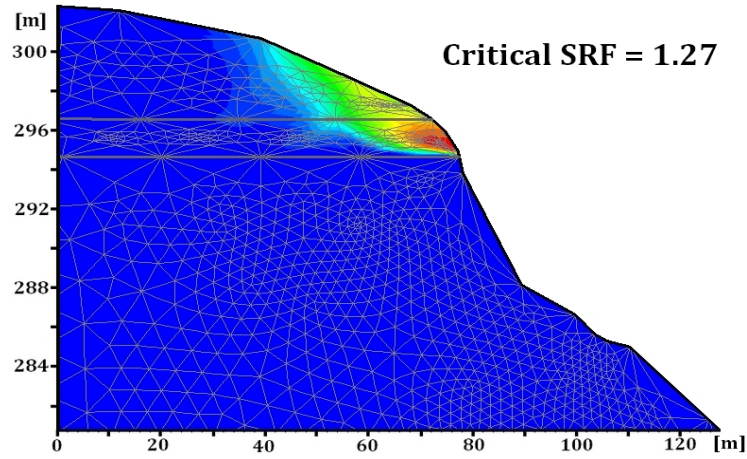
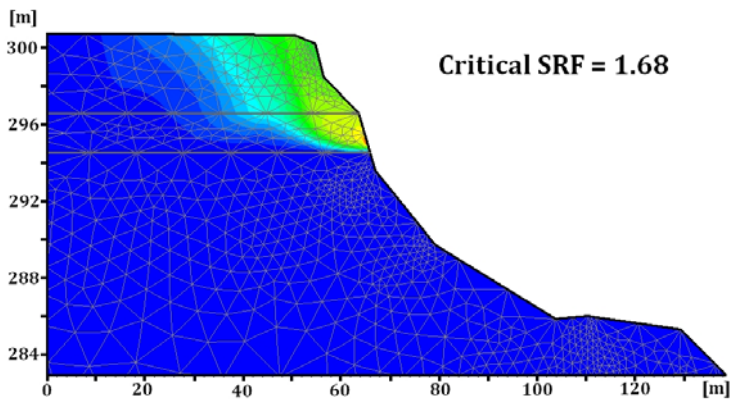


Figure 22. The results of the global stability analysis of the slope, total displacements are marked in blue to red

5 The Dips software was used for the kinematic analysis. The direction of the hillslopes and the direction of the discontinuities were compared to determine the location of the potential hazardous failure zones on the hillside. Possibility of planar sliding and wedge failure were analyzed. Toppling failure due to the geomorphology cannot occur. There was no regular spacing of the discontinuities. Stereographic plots were generated showing the possible failure planes for all slope directions. As an example the most hazardous part of the slope is shown here (75/75) (Fig. 23.). The safety factor of the possible sliding rock (planar failure) was calculated by Rocplane software (Fig. 24).

10

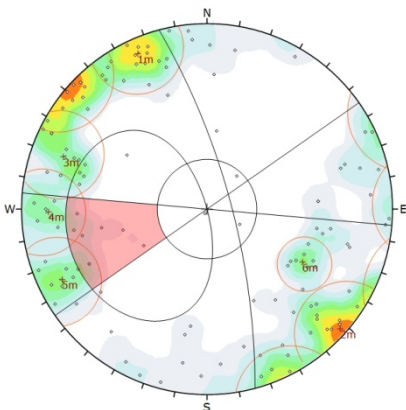


Figure 23. Kinematic analysis of planar failure (slope: 75/75)

15

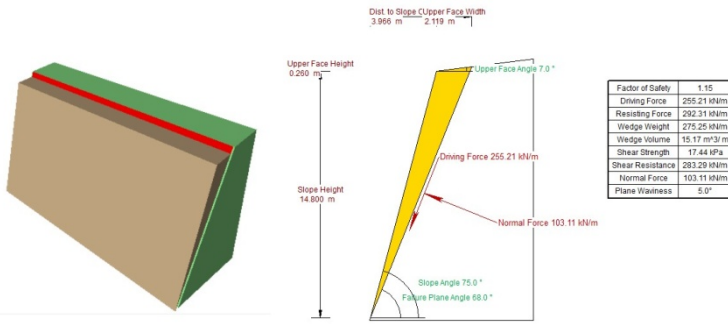


Figure 24. Analysis of planar failure by Rocplane (slope: 75/75)

The mechanism of wedge failure was also analyzed. Three possible wedge failure modes were identified as being the most hazardous (Fig. 25). The safety factors of the stability of wedges were calculated with the Swedge software (Fig. 26-28).

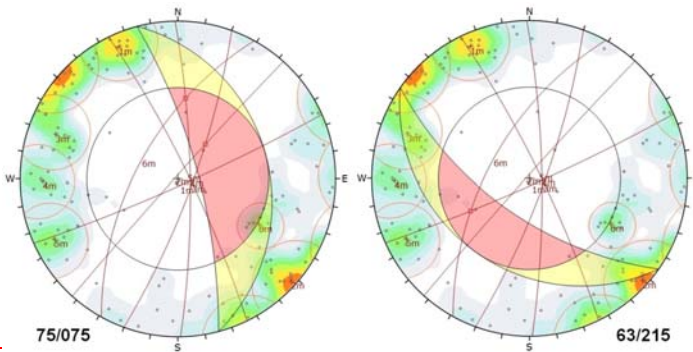


Figure 25. Examples for the kinematic analysis of wedge failure

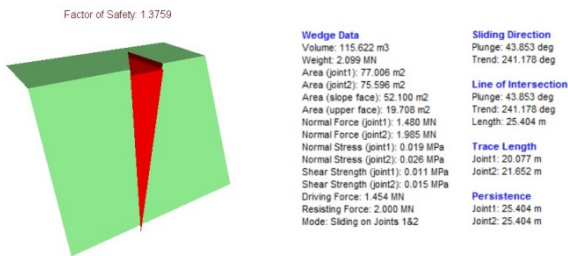


Figure 26. Analysis and graphic representation of wedge failure—type 1

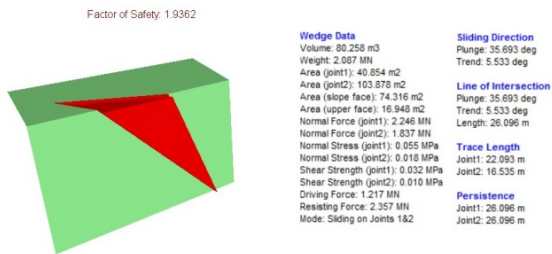


Figure 27. Analysis and graphic representation of wedge failure—type 2

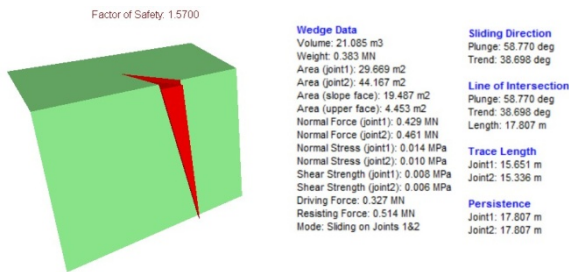


Figure 28. Analysis and graphic representation of wedge failure—type 3

4.5. Surface model resolution and engineering geological applicability of RPAS

There are three critical sets of input data in modelling of rocky slopes: i) slope geometry, ii) strength of rock mass and iii) joints system. To obtain the first—the slope geometry traditional surveying techniques were used but when the cliff is hardly accessible, these techniques do not provide appropriate data. Thus, the application of new methods such as RPAS or TLS can help to overcome this problem. The required resolution for slope stability modelling is in the order of 10 cm, rarely 1 cm. Both techniques allow having such highly precise geometries. The drawback of these techniques is that data acquisition is a rapid process but data management and model generation take time. It has been suggested that low cost RPAS can be used in rockfall scenario analysis (Giordan et al. 2015). The combination of RPAS and TLS can also be used for fine scale modelling of erosion (Neugirg 2016). In this study, the generation of DTM and rock slope profiles were crucial for slope stability analysis. It was not possible to obtain slope morphology by using any other method. For the determination of the strength of rock masses, we first used Schmidt hammer on site. But our field tests indicate that the application of Schmidt hammer in rock strength analysis is limited when it comes to the analysis of weak low strength rocks, such as volcanic tuff. As a consequence, laboratory analysis of samples was required to obtain reliable strength parameters. The documentation of joint system and discontinuity surfaces was first made based on field data. The measurements survey provided reliable data on joint orientation; however, the joint system that was found on inaccessible cliffs was not detectable. To overcome this problem, RPAS and TSL generated images were used. The frequency of joints was observed based on these images. Similar approach was used like in previous studies by Assali et al. (2014), Martino & Mazzanti (2014) and Margottini et al. 2015. It is necessary to emphasize that with the sole use of these remote sensing techniques, it is not possible to detect precise (2015). The required resolution for joint orientation. Consequently, field measurements are considered a must frequency is in joint system analysis.

This research has proved that the terrestrial laser scanning can achieve highly detailed and high precision point cloud about the studied surface. This point cloud is an excellent base to the elevation model, where suitable morphology analysis tools can draw the geologists' attention to the places where further examinations shall be performed.

The remotely piloted aircraft system is a relatively new platform in earth sciences (, but it has become clear that the captured imagery can be processed in a closed technology resulting in a point cloud, all order of which is comparable to the TLS based one. The resolution and quality of the obtained point cloud has been evaluated in the corresponding steps: digital elevation model and morphological analyses have been executed in the same manner as it was done with TLS data. It can be stated that the outcome of the 10 cm, rarely 1 cm. The RPAS data capture and processing technology is similarly useful for geological applications.

5. Conclusions

The application of terrestrial laser scanning and remotely piloted aircraft system is an excellent field data capturing technique for stability assessment of steep rock slopes. If the focus is on hazard evaluation, these technologies must be deployed very quickly, the data must be available in an easy and rapid way, and of course, the achieved information must support the required geoanalysis methods. The present study of highly dissected slope also proves that TLS is a technology where

inaccessible terrain parts can result in completeness problems. The use of RPAS technique can overcome this bottleneck: by the application of UAVs equipped with camera, relevant amount and quality imagery data can be collected about steep cliff faces. If no physical approach of a cliff is needed the field work is much safer; this technology can support even the documentation and evaluation of life threatening locations. The vegetation cover hides some part of the surface, but choosing adequate data acquisition time (e.g. in canopy free seasons), this circumstances can be managed. The collected images also provide a visual base to interpret the phenomena affecting the surface deformations. The remote sensing techniques applied provide key data on slope geometries. Without obtaining slope geometries the FEM modelling of slope is impossible. Beside slope geometries, the joint system can also be detected by TLS and RPAS. These techniques provide data mostly on joint spacing. Hence, the field documentation of joints is crucial in detecting joint orientation. In addition to those drawbacks, at dissected and shaded areas where data gathering is not reliable, completeness problems may arise. Laboratory analyses of rock types are also necessary to obtain reliable geomechanical input parameters for the FEM model. Thus the slope stability analysis of steep rock slopes requires the use of these combined methods. allows having plane surface geometries, however many joints are not plane surfaces and there are hardly visible sets in shadows. Thus RPAS can be used to outline the strike of major joints, but it might causes problem when it comes to the determination of dip and the displacement along the fault planes (e.g. slickensides).

For the determination of the strength of rock masses, we first used Schmidt hammer on site, which is a common practice (Margottini et al. 2015). Our field tests indicate that the application of Schmidt hammer in rock strength analysis is limited when it comes to the analysis of low strength rocks, such as volcanic tuff (Aydan & Ulusay 2003). As a consequence, laboratory analyses of samples were also required to obtain reliable strength parameters. To measure the strength and to understand the weathering characteristics, samples were taken representing different stratigraphic positions. Our lab test data (Table 2) clearly indicates that a low strength unit is found in the studied sections (unit marked by 'B-D' on Fig 8). Whether the low strength of this zone is related to differential weathering or it is associated with inherited weakness (micro-fabric) is not clear. Our results are in good correlations with the previous findings since this volcanic tuff was proved to be very prone to weathering. A loss in tensile strength of 60% was measured under simulated laboratory conditions (Stück et al. 2008). Weathering processes have been long known to induce landslides and cause slope stability problems in various lithologies and especially pyroclastic rocks (Chigra 2002, Fanti et al. 2013). At the studied rhyolite tuff cliff face it was shown that joint system is responsible for slope instabilities: planar and wedge failures were found (Fig. 9., Fig. 10). It is in agreement in several previous works, where the structural geological control of slope stability of highly dissected cliffs was pointed out (Agliardi et al. 2013, Fanti et al. 2013, Feng et al. 2014).

Comparison of surveying techniques obtaining of slope geometry and terrain model data for slope stability analysis helps to choose the appropriate technique (Table 3).

The professional routine is mostly required for classical tachymetry, where the surveyors need to have geological knowledge and surveying expertise to collect the most relevant points. This technology operates usually by the lowest number of measured points, so their quality and distribution is therefore very crucial. The TLS of nowadays are in counterpart very fast instruments (Assali et al. 2014, Neugrig et al. 2016) capturing high amount of terrain points with the ease like using smart phones. Image capture by RPAS is fairly easy; time dependent automatic image capture (e.g. shoot in every second) allows to obtain reliable data. These cameras are mostly equipped by automatic exposure control, which are similar to pocket camera use. One of the drawbacks is that flying requires expertise in flight planning and/or manual operator control. Thanks to onboard electronics, the fastest data capturing method is the RPAS-based. This feature is advantageous if the object availability is limited or the objects are moving/changing. Surveying is the slowest solution to acquire the points, but the data processing is similarly fast (Table 3). TLS and RPAS collected data oblige more processing time – sometimes it is computational hardware dependent. The most homogenous data is obtained by the RPAS methodology; tachymetry can be

applied also in this manner, although the efficiency is then very poor (Table 3). TLS has a typical circular pattern having decreasing point density. By corresponding resampling and/or interpolation this drawback can be eliminated. The highest spatial resolution can be achieved by TLS (Table 3). The spatial resolution of RPAS depends on flying time and object distance. Tachymetry is generally a low resolution data collection way. Because tachymeters and laser scanners must stand on the terrain, these technologies are highly dependent from terrain accessibility (slope steepness, vegetation), which is very advantageous for RPAS-based technology (Table 3). RPAS is similarly very robust on shadowing effects, caused by vegetation or other objects. The cost estimations for the given technologies were compiled by the experience taken from the literature. Excellent comparisons and evaluations can be found in Eisenbeiss & Zhang 2006, Koma et al. 2014, Milenkovic et al 2016, Naumann et al. 2013, Rothmund et al. 2013. The data set suggests that on average the costs of RPAS survey are lower than that of TLDS and tachmietry (Table 3).

Table 3. Comparison of the applicability of RPAS-based technology with terrestrial laser scanning (TLS) and tachymetry for rock slope stability assessment. Time frames and applicability is marked by '+' while costs are shown by '\$'

| | <u>RPAS</u> | <u>TLS</u> | <u>Tachymetry</u> |
|--|-------------|-----------------|----------------------|
| <u>Required expertise</u> | <u>++</u> | <u>+</u> | <u>+++</u> |
| <u>Data capturing speed on site (number of obtained data points)</u> | <u>+++</u> | <u>++</u> | <u>+</u> |
| <u>Required data processing time</u> | <u>++</u> | <u>++</u> | <u>+</u> |
| <u>Homogeneity of collected data</u> | <u>+++</u> | <u>++</u> | <u>+ / +++ / +++</u> |
| <u>Resolution</u> | <u>++</u> | <u>+++</u> | <u>+</u> |
| <u>Difficulty caused by slope accessibility</u> | <u>+</u> | <u>++</u> | <u>++</u> |
| <u>Digital terrain modelling</u> | <u>+++</u> | <u>+++</u> | <u>+</u> |
| <u>Slope geometry</u> | <u>+++</u> | <u>+++</u> | <u>++</u> |
| <u>Joint system detection</u> | <u>+++</u> | <u>+++ / ++</u> | <u>+</u> |
| <u>Costs of surveying</u> | <u>\$</u> | <u>\$\$</u> | <u>\$\$\$</u> |
| <u>Costs of data processing</u> | <u>\$\$</u> | <u>\$\$</u> | <u>\$</u> |

+ low, ++ medium, +++ high, \$ low, \$\$ medium, \$\$\$ high

6. Conclusions

- The use of RPAS technique can overcome the bottleneck of detecting the geometries of highly dissected and inaccessible slopes. RPAS equipped with camera provides relevant amount and quality of imagery data on steep cliff faces.
- Comparing with TLS and tachymetry RPAS technique is much safer; cheaper, faster and provides excellent terrain model after data processing.
- Documentation of joints is essential for cliff face stability analysis. RPAS allows the detection of joint system (mainly strikes and partly dips but not slickensides) but field validation and field measurements of accessible joints and faults are recommended to justify joint orientation obtained from RPAS data based terrain models.
- The lithology and physical parameters of the studied steep cliffs are not uniform and intercalations of weak layers of vitric tuff and volcanoclastic breccia were found.
- According to 2D FEM modelling the intercalating low strength layer is the one where potential slip surface can develop causing larger scale mass movements, but at present it has low probability.
- Joint system has a crucial role in the stability of the studied rhyolite tuff cliff faces. The highest hazard is related to planar failure along ENE-WSW joints and to wedge failure.

Acknowledgements

The help of B. Czinder, B. Kleb, Z. Koppányi, B. Molnár, B. Pálincás and B. Vásárhelyi is acknowledged. The support of the National Research Development and Innovation (NKFI) Fund (ref. no. K 116532) is appreciated.

References

- 5 | Abbruzzese, J. M., ~~C.~~Sauthier, ~~and C.~~, Labiouse, V.: Considerations on Swiss methodologies for rock fall hazard mapping based on trajectory modeling. *Nat. Hazards Earth Syst. Sci.*, 9, 1095–1109, doi:10.5194/nhess-9-1095-2009, 2009.
- Agliardi, F., Crosta, G.B., Meloni, F., Valle, C., and Rivolta, C.: Structurally-controlled instability, damage and slope failure in a porphyry rock mass, *Tectonophysics* 605 (2013) 34–47, doi:10.1016/j.tecto.2013.05.033, 2013.
- 10 | Arikan, F., Ulusay, R. and Aydin, N.: Characterization of weathered acidic volcanic rocks and a weathering classification based on a rating system. *Bulletin of Engineering Geology and the Environment*, 66 (4): 415-430, 2007. doi:10.1007/s10064-007-0087-0, 2007.
- Assali, P., Grussenmeyer, P., Villemin, T., Pollet, N. and Viguier, F.: Surveying and ~~modeling~~**modelling** of rock discontinuities by terrestrial laser scanning and photogrammetry: Semi-automatic approaches for linear outcrop
15 | inspection. *J. of Struct. Geol.*, 66: 102-114, doi:10.1016/j.jsg.2014.05.014, 2014.
- Aydan, Ö., and Ulusay, R.: Geotechnical and environmental characteristics of man-made underground structures in Cappadocia, Turkey. *Eng. Geol.*, 69 (3/4): 245-272, doi:10.1016/S0013-7952(02)00285-5, 2003.
- [Balogh K.: Geological Formations of Bükk Mountains \(in Hungarian\), Annual Report of the Hungarian Geological Survey, 48\(2\), 245-719 1964.](#)
- 20 | [Brauneck, J., Pohl, R., Juepner, R.: Experiences of using UAVs for monitoring levee breaches. IOP Conf. Series: Earth and Environmental Science 46, 012046, IOP Publishing, doi:10.1088/1755-1315/46/1/012046, 2016.](#)
- Budetta, P.: Assessment of rockfall risk along roads, *Nat. Hazards Earth Syst. Sci.*, 4, 71–81, doi:10.5194/nhess-4-71-2004, 2004.
- ~~Chen, J., Dowman, I., Li, S., Li, Z., Madden, M., Mills, J., Pappadimitis, N., Rottensteiner, F., Sester, M., Toth, C., Trinder, J., Heipke, C. Information from imagery: ISPRS scientific vision and research agenda, *ISPRS Journal of Photogrammetry and Remote Sensing*, Vol. 115, pp. 3–21, doi:10.1016/j.isprsjprs.2015.09.008, 2016.~~
- 25 | ~~Choi, K., Lee, I., Hong, J., Oh, T., Shin, S.W., Developing a UAV-based rapid mapping system for emergency response. *The International Society for Optical Engineering (SPIE) Proceedings* 7332, 9–12, doi:10.1117/12.818492, 2009.~~
- ~~Casella, E., Rovere, A., Pedroncini, A., Stark, C. P., Casella, M., Ferrari, M., Firpo, M.: Drones as tools for monitoring beach topography changes in the Ligurian Sea (NW Mediterranean), *Geo-Marine Letters*, 36(2), 151-163., doi:10.1007/s00367-016-0435-9, 2016.~~
- 30 | ~~Chigira, M.: Geologic factors contributing to landslide generation in a pyroclastic area: August 1998 Nishigo Village, Japan. *Geomorphology*, Vol. 46(1-2), 117-128, doi:10.1016/S0169-555X(02)00058-2, 2002.~~
- Cloud Compare point cloud processing software (CC) available at: <http://www.cloudcompare.org/> (last access 1 February
35 | 2017), 2014
- ~~Colomina, I. and Molina, P. Unmanned aerial systems for photogrammetry and remote sensing: a review, *ISPRS Journal of Photogrammetry and Remote Sensing*, Vol. 92, pp. 79–97, doi: 10.1016/j.isprsjprs.2014.02.013, 2014.~~
- Conrad, O., Bechtel, B., Bock, M., Dietrich, H., Fischer, E., Gerlitz, L., Wehberg, J., Wichmann, V., and Böhner, J.: System for Automated Geoscientific Analyses (SAGA) v. 2.1.4, *Geosci. Model Dev.*, 8, 1991-2007, doi:10.5194/gmd-8-1991-
40 | 2015, 2015.

- Copons, R., Vilaplana, J. M., and Linares, R.: Rockfall travel distance analysis by using empirical models (Solà d'Andorra la Vella, Central Pyrenees), *Nat. Hazards Earth Syst. Sci.*, 9, 2107-2118, doi:10.5194/nhess-9-2107-2009, 2009.
- ~~Cramer, M. The UAV@LGL BW project — a NMCA case study. In: Fritsch, D. (Ed.) Photogrammetric Week 2013, Wichmann, pp. 151-16, 2013.~~
- 5 Crosta, G., and Agliardi, F.: How to obtain alert velocity thresholds for large rockslides. *Phys Chem Earth Parts ABC*. 27:1557-1565, doi:10.1016/S1474-7065(02)00177-8, 2002.
- Crosta, G. B., and Agliardi, F.: A methodology for physically based rockfall hazard assessment. *Natural Hazards and Earth System Sciences* 3: 407–422, doi:10.5194/nhess-3-407-2003, 2003.
- ~~D'Amato, J., Hantz, D., Guerin, A., Jaboyedoff, M., Baillet, L., and Mariscal, A.: Influence of meteorological factors on rockfall occurrence in a middle mountain limestone cliff . *Nat. Hazards Earth Syst. Sci.*, 16, 719-735, 2016. doi:10.5194/nhess-16-719-2016, 2016.~~
- 10 Danzi M., Di Crescenzo G., Ramondini M., Santo A. Use of unmanned aerial vehicles (UAVs) for photogrammetric surveys in rockfall instability studies, *Rend. Online Soc. Geol. It.*, Vol. XX, doi: 10.3301/Rol.2012.xx, 2013.
- De Biagi, V., Napoli, M.L., Barbero, M., and Peila, D.: Estimation of the return period of rockfall blocks according to their size. *Nat. Hazards Earth Syst. Sci.*, 17, 103–113, 2017, doi:10.5194/nhess-17-103-2017, 2017.
- 15 DJI phantom 2 quadcopter (DJI) available at: <http://www.dji.com/phantom-2> (last access 1 February 2017), 2015.
- Eisenbeiss, H. ~~The autonomous, Zhang, L. (2006): Comparison of DSMs generated from mini helicopter: A powerful platform for mobile mapping, The UAV imagery and terrestrial laser scanner in a cultural heritage application, International Archives of the Photogrammetry, Remote Sensing and Spatial Information Sciences, Vol. XXXVII, Part B1, Beijing, 2008., Volume XXXV/5, pp. 90-96~~
- 20 Fanti, R., Gigli, G., Lombardi, L., Tapete, D., Canuti, P., Terrestrial laser scanning for rockfall stability analysis in the cultural heritage site of Pitigliano (Italy). *Landslides* 10:409–420, DOI 10.1007/s10346-012-0329-5, 2013.
- ~~Faro Scene point cloud processing software (FaroScene) available at: <http://www.faro.com/en-us/products/faro-software/scene/overview> (last access 1 February 2017), 2012.~~
- 25 Faro terrestrial laser scanner (Faro) available at: <http://www.faro.com/en-us/products/3d-surveying/faro-focus3d/overview> (last access 1 February 2017), 2016.
- Feng, Z., Li, B., Yin, Y. P., and He, K.: Rockslides on limestone cliffs with subhorizontal bedding in the southwestern calcareous area of China. *Nat. Hazards Earth Syst. Sci.*, 14, 2627-2635, doi:10.5194/nhess-14-2627-2014, 2014.
- Francioni, M., Salvini, R., Stead, D., and Litrico, S.: A case study integrating remote sensing and distinct element analysis to quarry slope stability assessment in the Monte Altissimo area, Italy. *Eng. Geol.*, 183: 290-302., doi:10.1016/j.enggeo.2014.09.003, 2014.
- 30 ~~Fritz, A., Kattenborn, T., Koch, B., UAV based photogrammetric point clouds — tree stem mapping in open stands in comparison to terrestrial laser scanner point clouds. *ISPRS — Int. Arch. Photogramm. Remote Sens. Spatial Inform. Sci.*, 141–146. 2013.~~
- 35 ~~Fraštia, M., Marčiš, M., Kopecký, M., Liščák, P., Žilka, A.: Complex geodetic and photogrammetric monitoring of the Kralovany rock slide. *Journal of Sustainable Mining*, 13(4), 12–16. doi: 10.7424/jsm140403, 2014.~~
- Geomagic Design X 3D modelling software (GeomagicDesignX) available at: <http://www.geomagic.com/en/products-landing-pages/designx> (last access 1 February 2017), 2016
- Geomagic Studio 3D modelling software (GeomagicStudio) available at: <http://www.geomagic.com/en/> (last access 1 February 2017), 2013
- 40 Giordan, D., Manconi A., Allasia P., and Bertolo D.: Brief Communication: On the rapid and efficient monitoring results dissemination in landslide emergency scenarios: the Mont de La Saxe case study. *Nat. Hazards Earth Syst. Sci.*, 15, 2009–2017, 2015, oi:10.5194/nhess-15-2009-2015, 2015.

GoPro action cam (GoPro) available at: <https://gopro.com/> (last access 1 February 2017), 2017

~~Grenzdörffer, G.J., UAS based automatic bird count of a common gull colony. ISPRS—Int. Arch. Photogramm. Remote Sens. Spatial Inform. Sci. XL-1/W2, 169–174, 2013.~~

Haas, F., Hilger, L., Neugirg, F., Umstädter, K., Breitung, C., Fischer, P., Hilger, P., Heckmann, T., Dusik, J., Kaiser, A., Schmidt, J., Della Seta, M., Rosenkranz, R., and Becht, M.: Quantification and analysis of geomorphic processes on a recultivated iron ore mine on the Italian island of Elba using long-term ground-based lidar and photogrammetric SfM data by a UAV, *Nat. Hazards Earth Syst. Sci.*, 16, 1269–1288, doi:10.5194/nhess-16-1269-2016, 2016.

~~Harwin, S., Lucieer, A. Assessing the accuracy of georeferenced point clouds produced via multi-view stereopsis from unmanned aerial vehicle (UAV) imagery. Remote Sens. 4, 1573–1599, doi: 10.3390/rs4061573, 2012.~~

Hoek, E., Carranza-Torres, C., and Corkum, B.: Hoek-Brown failure criterion – 2002 Edition. Proc. NARMS-TAC Conference, Toronto, 1, 267–273, 2002.

~~Hudson, J.A., Harrison, J.P. Engineering rock mechanics: an introduction to the principles, Pergamon Press, 1997, p444.~~

Inverse distance weighting interpolation (IDW) available at: <http://gisgeography.com/inverse-distance-weighting-idw-interpolation/> (last access 1 February 2017), 2013

~~Kaşmer, Ö., Ulusay R., and Geniş, M. Assessments on the stability of natural slopes prone to toe erosion, and man-made historical semi-underground openings carved in soft tuffs at Zelve Open Air Museum (Cappadocia, Turkey), Engineering Geology 158 (2013) 135–158, doi:10.1016/j.enggeo.2013.03.010, 2013.~~

~~Kostrzewa, J., Meyer, W., Laband, S., Terre, W., Petrovich, P., Swanson, K., Sundra, C., Sener, W., Wilmott, J. Infrared microsensor payload for miniature unmanned aerial vehicles. In: Proc. SPIE 5090, Unattended Ground Sensor Technologies and Applications, vol. 265, doi: 10.1117/12.500712. 2003.~~

~~Jovančević, S. D., Peranić, J., Ružić, I. and Arbanas, Ž.: Analysis of a historical landslide in the Rječina River Valley, Croatia. Geoenvironmental Disasters, 3:26, doi:10.1186/s40677-016-0061-x, 2016.~~

~~Koma, Zs., Székely, B., Dorninger, P., Rasztoivts, S., Roncat, A., Zámolyi, A., Krawczyk, D., Pfeifer, N. (2014): Comparison of UAV and TLS DTMs for acquisition of geological, geomorphological information for Doren landslide, Vorarlberg Austria, EGU General Assembly Conference Abstracts, 2014~~

LAS laser scanner point cloud datatype specification (LAS) available at: <https://www.asprs.org/committee-general/laser-las-file-format-exchange-activities.html> (last access 1 February 2017), 2012

Leica CS10 controller (CS10) available at: <http://leica-geosystems.com/products/gnss-systems/controllers/leica-viva-cs15-and-cs10> (last access 1 February 2017), 2014

Leica Cyclone point cloud processing software (LeicaCyclone) available at: <http://leica-geosystems.com/products/laser-scanners/software/leica-cyclone> (last access 1 February 2017), 2016

Leica GNSS receiver (GS08) available at: <http://leica-geosystems.com/products/gnss-systems/smart-antennas/leica-viva-gs08plus> (last access 1 February 2017), 2014

~~Lindner, G., Schraml, K., Mansberger, R., and Hübl, J.: UAV monitoring and documentation of a large landslide. Appl Geomat 8:1–11, doi:10.1007/s12518-015-0165-0, 2016.~~

~~Liu, T., Deng, J., Zheng, J., Zhengd, L., Zhang, Z., and Zheng, H.: A new semi-deterministic block theory method with digital photogrammetry for stability analysis of a high rock slope in China, Engineering Geology 216 (2017) 76–89, doi:10.1016/j.enggeo.2013.03.010, 2017.~~

Lowe, D.G. (2004): *International Journal of Computer Vision* 60: 91, doi: 10.1023/B:VISI.0000029664.99615.94

Manconi, A., and Giordan, D.: Landslide failure forecast in near-real-time, *Geomatics, Natural Hazards and Risk*, 2014, doi:10.1080/19475705.2014.942388, 2014.

Manconi, A., and Giordan, D.: Landslide early warning based on failure forecast models: the example of the Mt. de La Saxe rockslide, northern Italy. *Nat. Hazards Earth Syst. Sci.*, 15, 1639–1644, 2015, doi:10.5194/nhess-15-1639-2015, 2015.

- Margottini, C., Antidze, N., Corominas, J., Crosta, G.B., Frattini, P., Gigli, G., Giordan, D., Iwasaky, I., Lollino, G., Manconi, A., Marinou, P., Scavia, C., Sonnessa, A., Spizzichino, D., and Vacheishvili, N.: Landslide hazard, monitoring and conservation strategy for the safeguard of Vardzia Byzantine monastery complex, Georgia. *Landslides* 12:193–204, doi:10.1007/s10346-014-0548-z, 2015.
- 5 Marinou, V., Marinou, P., and Hoek, E.: The geological strength index: applications and limitations. *Bull Eng Geol Environ* 64: 55–65, doi:10.1007/s10064-004-0270-5, 2005.
- Martino, S., and Mazzanti, P.: Integrating geomechanical surveys and remote sensing for sea cliff slope stability analysis: the Mt. Pucci case study (Italy). *Nat. Hazards Earth Syst. Sci.*, 14, 831-848, doi:10.5194/nhess-14-831-2014, 2014.
- Mateos, R.M., García-Moreno, I., Reichenbach, P., Herrera, G., Sarro, R., Rius, J., Aguiló, R., and Fiorucci, F.: Calibration and validation of rockfall modeling at regional scale: application along a roadway in Mallorca (Spain) and organization of its management. *Landslides* 13:751–763, doi:10.1007/s10346-015-0602-5, 2016.
- 10 Mathworks Matlab mathematical environment (Matlab) available at: <https://www.mathworks.com/products/matlab.html>, (last access 1 February 2017), 2017
- Michoud, C., Derron, M.-H., Horton, P., Jaboyedoff, M., Baillifard, F.-J., Loye, A., Nicolet, P., Pedrazzini, A., and Queyrel, A.: Rockfall hazard and risk assessments along roads at a regional scale: example in Swiss Alps. *Nat. Hazards Earth Syst. Sci.*, 12, 615–629, 2012. doi:10.5194/nhess-12-615-2012, 2012.
- 15 ~~Muceku, Y., Korini, O., and Kuriqi, A.: Geotechnical Analysis of Hill's Slopes Areas in Heritage Town of Berati, Albania. *Period. Polytech. Civil Eng.*, (60)1, 61–73, 2016. doi:10.3311/PPei.7752, 2016.~~
- ~~Milenkovic, M., Karel, W., Ressler, C., Pfeifer, N.: A comparison of UAV and TLS data for soil roughness assessment, *ISPRS Annals of the Photogrammetry, Remote Sensing and Spatial Information Sciences*, Volume III-5, pp. 145-152, doi:10.5194/isprsannals-III-5-145-2016, 2016.~~
- ~~Naumann, M., Geist, M., Bill, R., Niemeyer, F., Grenzdörffer, G.: Accuracy comparison of digital surface models created by unmanned aerial systems imagery and terrestrial laser scanner, *International Archives of the Photogrammetry, Remote Sensing and Spatial Information Sciences*, Volume XL-1/W2, pp. 281-286, 2013.~~
- 25 Neugirg, F., Stark, M., Kaiser A., Vlacilova M., Della Seta M., Vergari F., Schmidt J., Becht M, Haas F. Erosion processes in calanchi in the Upper Orcia Valley, Southern Tuscany, Italy based on multitemporal high-resolution terrestrial LiDAR and UAV surveys. *Geomorphology*, 269, 8-22. doi: 10.1016/j.geomorph.2016.06.027, 2016.
- Niethammer, U., James, M.R., Rothmund, S., Travelletti, J., Joswig, M. UAV-based remote sensing of the Super-Sauze landslide: Evaluation and results. *Engineering Geology* 128, 2-11, doi: 10.1016/j.enggeo.2011.03.012, 2012.
- 30 ~~Pajares, G. Overview and current status of remote sensing applications based on unmanned aerial vehicles, *Photogrammetric Engineering and Remote Sensing*, 81, 4, 281–329, doi: 10.14358/PERS.81.4.197, 2015.~~
- Pappalardo, G., Mineo, S., and Rapisarda, F.: Rockfall hazard assessment along a road on the Peloritani Mountains (northeastern Sicily, Italy) *Nat. Hazards Earth Syst. Sci.*, 14, 2735-2748, doi:10.5194/nhess-14-2735-2014, 2014.
- ~~Park, H. J., Lee, J. H., Kima, K. M., and Umb, J. G.: Assessment of rock slope stability using GIS based probabilistic kinematic analysis, *Engineering Geology* 203, 56–69., doi:10.1016/j.enggeo.2015.08.021, 2016.~~
- 35 Pix4D photogrammetry software (Pix4D) available at: <https://pix4d.com/product/pix4dmapper-pro/> (last access 1 February 2017), 2017
- Rau, J., Jhan, J., Lob, C., Linb, Y. Landslide mapping using imagery acquired by a fixed-wing UAV. *ISPRS – Int. Arch. Photogramm. Remote Sens. Spatial Inform. Sci.* XXXVIII-1/C22, 195–200, 2011.
- 40 Real time kinematic net service (RTKnet) available at: <https://www.gnssnet.hu> (last access 1 February 2017), 2013
- ~~Rinaudo, F., Chiabrando, F., Lingua, A., Span, A. Archaeological site monitoring: UAV photogrammetry can be an answer. *ISPRS – Int. Arch. Photogramm. Remote Sens. Spatial Inform. Sci.* XXXIX-B5, 583–588, 2012.~~

- ~~Rufino, G., Moccia, A., Integrated VIS-NIR-Hyperspectral/thermal IR-Electrooptical Payload System for a Mini UAV. American Institute of Aeronautics and Astronautics, Arlington, VA, USA, pp. 647–664, 2005.~~
- ~~Rothmund, S., Niethammer, U., Walter, M., Joswig, M.: Comparison of DSMs acquired by terrestrial laser scanning, UAV-based aerial images and ground-based optical images at the Super-Sauze landslide, EGU General Assembly Conference Abstracts, 2013.~~
- 5 Samodra, G., Chen, G., Sartohadi, J., Hadmoko, D.S., Kasama, K., and Setiawan, M.A.: Rockfall susceptibility zoning based on back analysis of rockfall deposit inventory in Gunung Kelir, Java. *Landslides* (2016) 13:805–819, doi:10.1007/s10346-016-0713-7., 2016.
- ~~Scholtz, A., Kasechwich, C., Kruger, A., Kufieta, K., Schnetter, P., Wilkens, C., Kruger, T., Vorsmann, P. Development of a new multi purpose UAS for scientific application. ISPRS—Int. Arch. Photogramm. Remote Sens. Spatial Inform. Sci. XXXVIII 1/C22, 149–154, 2011.~~
- ~~Shamekhi, E., and Tannant, D.D.: Probabilistic assessment of rock slope stability using response surfaces determined from finite element models of geometric realizations, Computers and Geotechnics 69, 70–81., doi: 10.1016/j.compgeo.2015.04.014, 2015.~~
- 10 ~~Spreafico M.C., Perotti L., Cervi F., Bacenetti M., Bitelli G., Girelli V.A., Mandanici E., Tini M.A., Borgatti L. Terrestrial Remote Sensing techniques to complement conventional geomechanical surveys for the assessment of landslide hazard: The San Leo case study (Italy) European Journal of Remote Sensing 2015, 48, pp. 639–660, doi: 10.5721/EuJRS20154835, 2015.~~
- 15 ~~Stead, D. Wolter A. A critical review of rock slope failure mechanisms: The importance of structural geology. J. Structural Geology, 74, 1-23. doi: 10.1016/j.jsg.2015.02.002, 2015.~~
- 20 ~~Stück, H., Forgó, L.Z., Rüdrieh, J., Siegesmund, S., Török, Á.: The behaviour of consolidated volcanic tuffs: weathering mechanisms under simulated laboratory conditions, Environmental Geology, Vol. 56(3-4), 699-713, doi:10.1007/s00254-008-1337-6, 2008.~~
- ~~Török, Á., Forgó, L.Z. Vogt, T., Löbens, S., Siegesmund, S., and Weiss, T.: The influence of lithology and pore-size distribution on the durability of acid volcanic tuffs, Hungary. Prykriil, R. & Smith, J.B. (Eds.): Building Stone Decay: From Diagnosis to Conservation, Geological Society, London, Special Publications 271: 251-260, 2007.~~
- 25 ~~Tuckey, Z., and Stead, D.: Improvements to field and remote sensing methods for mapping discontinuity persistence and intact rock bridges in rock slopes, Engineering Geology 208 (2016) 136–153, doi:10.1016/j.enggeo.2016.05.001, 2016.~~
- ~~Westoby M.J., Brasington J., Glasser N.F., Hambrey M.J., Reynolds J.M. Structure-from-Motion’ photogrammetry: A low-cost, effective tool for geoscience applications, Geomorphology, Volume 179, Elsevier, pp. 300–314, doi: 10.1016/j.geomorph.2012.08.021, 2012.~~
- 30 ~~Wich, S., Koh, L., Conservation drones: the use of unmanned aerial vehicles by ecologists. GIM Int. 26, 29–33. 2012.~~
- ~~Z+F terrestrial laser scanner (Z+F) available at: http://www.zf-laser.com/Z-F-IMAGER-R-5010C.3d_laserscanner.0.html?&L=1 (last access 1 February 2017), 2014.~~